

AD-A090 783

VARIAN ASSOCIATES INC PALO ALTO CA

F/6 9/5

5 KW, CW LOW LOSS BOOSTER TUBE FOR MILITARY SATCOM SYSTEMS. (U)

DAA807-77-C-0010

NL

UNCLASSIFIED

1 CP 1
AD-9
090783

END
DATE FILMED
11-80
DTIC

AD A090783



①

LEVEL II

**5 kW, CW LOW LOSS BOOSTER TUBE
for
MILITARY SATCOM SYSTEMS**

Final Technical Report for Contract No. DAAB07-77-C-0010

October 1978

Prepared by:

B. G. James

Varian Associates, Inc.

*611 Hansen Way
Palo Alto, California 94303*



F

DDC FILE COPY

ECOM

US ARMY ELECTRONICS COMMAND
FORT MONMOUTH, NEW JERSEY

Approved for public release by the Defense Dept.
Distribution is unlimited.

80 10 23 026

5 kW, CW LOW LOSS BOOSTER TUBE
for
MILITARY SATCOM SYSTEMS,

Final Technical Report for Contract No. DAAB07-77-C-0010 Rev

11/5 October 1978

141

Per
letter on file

Prepared by:
B. G. James

Approved by:
Available
Dist. F

A

Varian Associates, Inc.
611 Hansen Way
Palo Alto, California 94303

70 00 00 00

30 11/01

TABLE OF CONTENTS

<u>Section</u>		<u>Page</u>
I.	INTRODUCTION.....	1
II.	ELECTRICAL DESIGN.....	2
	A. Electron Gun.....	2
	B. Circuit.....	3
	C. Stability.....	6
III.	TEST DATA.....	14

LIST OF ILLUSTRATIONS

<u>Figure</u>		<u>Page</u>
1.	Cross-Sectional View of the Final Gun Design.....	4
2.	Small Signal Gain Calculations.....	5
3.	Twelve-Cavity Design -- Power vs Frequency.....	7
4.	Twelve-Cavity Design -- Gain vs Frequency.....	8
5.	Transmission Insertion Loss.....	9
6.	Match Data.....	10
7.	Stability Calculations, 12- and 14-Cavity Design.....	13
8.	Output Power vs 7.9-8.0 Frequency.....	16
9.	Output Power vs 8.0-8.1 Frequency.....	17
10.	Output Power vs 8.1-8.2 Frequency.....	18
11.	Output Power vs 8.2-8.3 Frequency.....	19
12.	Output Power vs 8.3-8.4 Frequency.....	20
13.	Power Output vs Power Drive -- 7.9 GHz.....	21
14.	Power Output vs Power Drive -- 8.0-8.05 GHz.....	22
15.	Power Output vs Power Drive -- 8.1, 8.15, 8.2 GHz.....	23
16.	Power Output vs Power Drive -- 8.2, 8.25 GHz.....	24
17.	Power Output vs Power Drive -- 8.3, 8.35, 8.4 GHz.....	25
18.	Booster Amplitude Measured with Klystron Driver 7.9-8.0 Frequency.....	26
19.	Booster Amplitude Measured with Klystron Driver 8.0-8.1 Frequency.....	27
20.	Booster Amplitude Measured with Klystron Driver 8.1-8.2 Frequency.....	28
21.	Booster Amplitude Measured with Klystron Driver 8.2-8.3 Frequency.....	29
22.	Booster Amplitude Measured with Klystron Driver 8.3-8.4 Frequency.....	30

LIST OF ILLUSTRATIONS (Cont.)

<u>Figure</u>		<u>Page</u>
23.	Booster Phase Deviation from Linearity Measured with Klystron Driver 7.0-8.0 Frequency.....	31
24.	Booster Phase Deviation from Linearity Measured with Klystron Driver 8.0-8.1 Frequency.....	32
25.	Booster Phase Deviation from Linearity Measured with Klystron Driver 8.1-8.2 Frequency.....	33
26.	Booster Phase Deviation from Linearity Measured with Klystron Driver 8.2-8.3 Frequency.....	34
27.	Booster Phase Deviation from Linearity Measured with Klystron Driver 8.3-8.4 Frequency.....	35
28.	Stability Calculations.....	36

I. INTRODUCTION

This report describes the work performed on Contract DAAB07-77-C-0010 for the U.S. Army Electronics Command. The report documents the development of a low loss single section coupled cavity traveling wave tube designated as a Booster Tube which may be used in military satellite communication ground terminals.

The primary objective of the program was to design, fabricate and test a prototype tube which would deliver 5 kW of CW power in the frequency band of 7.9 - 8.4 GHz with 10 dB of saturated gain and low insertion loss.

The first task on the program was the modification of a design previously tested at a higher power level and the analytical optimization of this design. This was followed by the fabrication of test circuits for cold rf testing. An electron gun was designed with a modulating anode and tested in the beam analyzer. These tasks then led to the design and construction of a prototype tube.

The tube was tested using a high power klystron as a driver. The klystron was tuned in 100 MHz steps across the band and the power, gain, amplitude phase and stability were measured. These data are presented in the contents of this report.

II. ELECTRICAL DESIGN

A. ELECTRON GUN

A gun using a modulating anode for control of the beam current was selected for the tube. The modulating anode is used to allow the booster tube to be cut off during normal feed-through operation. When the system requires an additional 10 dB of power output, the modulating anode is then switched to ground potential turning the tube on to full beam power.

The most difficult task in the gun design is to obtain the required shape of the magnetic polepiece and anode while maintaining the required spacings for arc-free performance. The magnetic polepiece was designed for confined flow focusing. This means that the magnetic field lines should closely follow the electrostatic electron trajectories in the cathode-anode region.

The performance of a traveling wave tube is critically dependent on the beam size. The effective diameter determining the interaction between the beam and circuit is close to the 50% point in current density distribution. The largest possible effective beam filling factor is desired for high gain and conversion efficiency.

A design goal of 5% beam ripple was selected. In order that this percentage of ripple be achieved in the design and still maintain the gun electrode spacing for arc-free performance, a gun coil was added in the solenoid design. This gun coil shapes the magnetic flux lines in the gun region to launch the beam into the main uniform magnetic field with minimum ripple.

The gun was designed by first using computer calculations. The computer employs a relaxation technique to calculate the potential, including effects of space charge. Based on this potential, electron trajectories are calculated with and without magnetic field. The computer model injects electrons with the correct density and velocity. The electrode shapes are then altered until the desired beam is obtained. The design goal is fairly uniform spacings of the electron trajectories along the beam path, but especially near the beam minimum.

A gun model is assembled and operated in the beam analyzer. The beam analyzer results are compared to the computed results, and the electrode shapes are altered, if necessary, to improve gun performance. When a good electrostatic beam is obtained in the beam analyzer, the magnetic field is applied and the shape adjusted to acquire a low value of beam ripple.

The beam analyzer measures the current density across the beam at a number of axial positions, starting from the magnetic aperture near the anode and extending down the uniform region of magnetic field. These measurements give the exact behavior of the gun and beam in terms of average beam ripple.

The beam profiles measured on the final gun design are extremely good. With the use of the gun coil, a minimum of 2% of beam scalloping was achieved. Figure 1 shows a cross-sectional view of the gun.

B. CIRCUIT

The circuit design for the tube was accomplished by scaling the higher power tube design described in Varian Technical Proposal No. 76-30137 dated April 1976.

The circuit design scaling was accomplished by computer calculations. Both small signal and large signal calculations were carried out.

Figure 2 shows the calculated small signal gain for the booster tube. The calculations were carried out for two circuit sections, a twelve-cavity section and a fourteen-cavity section. The twelve-cavity section operating at 13.5 kV at a beam current of 2.0 A had an average gain of 17 dB but rolled off at the upper band edge to 15 dB.

The fourteen-cavity circuit operating at 13 kV and 1.6 A of beam current produced a well balanced gain over the band with a minimum gain at 18 dB at the band edges and 19.6 dB at band center.

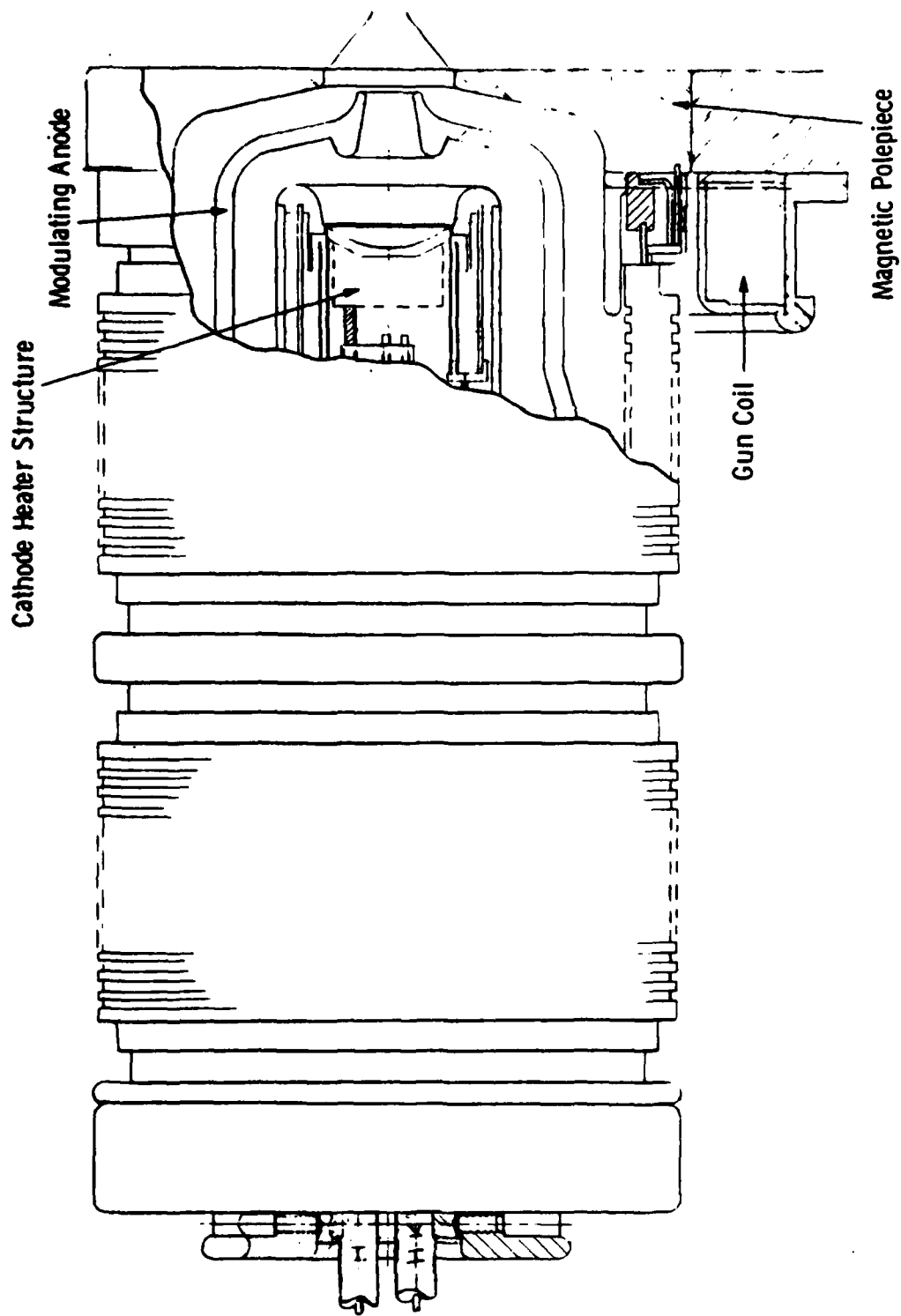


Figure 1. Cross-Sectional View of the Final Gun Design

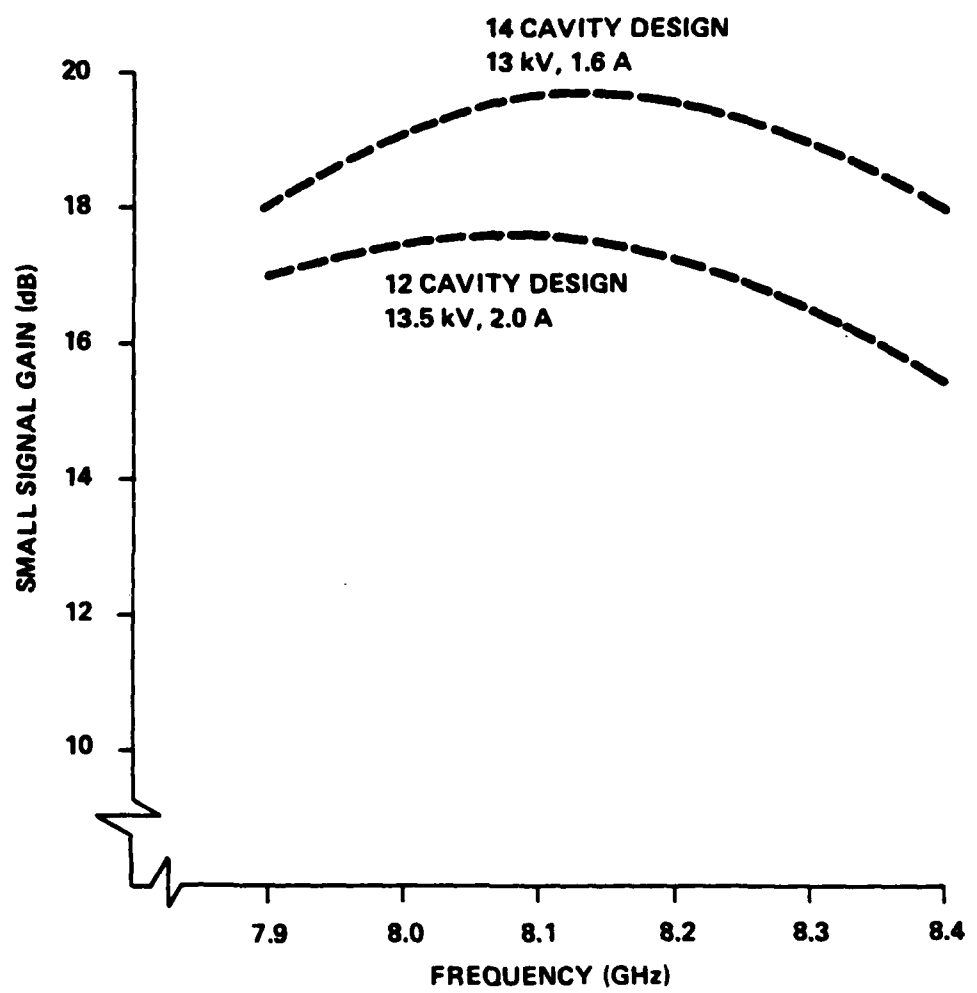


Figure 2. Small Signal Gain Calculations

Large signal calculations were carried out on the twelve-cavity circuit to find the power output capability of this circuit design, and the large signal gain expected.

Figure 3 shows the power output calculated as a function of frequency and by varying the drive power in 3 dB steps starting at 100 W. The calculations show that the tube had adequate power to meet the 5 kW CW requirements at 400 W drive.

Figure 4 shows the large signal gain behavior of the tube at various drive powers. These calculations were again carried out with a beam voltage of 13.5 kV and a beam current of 2 A. As can be seen at the 400 W level of rf drive, the large signal gain meets the 10 dB required goal.

Based on the calculations carried out, a thirteen-cavity booster tube was designed and constructed. The choice of using thirteen cavities instead of twelve or fourteen was because of waveguide considerations in the solenoid.

Figure 5 shows the transmission insertion loss measured on the tube. As can be seen, the insertion loss measured over the band of interest is approximately 0.9 dB. This insertion loss measurement includes reflections from the circuit and transitions.

Figure 6 shows the match data achieved on the tube looking through both waveguide transitions. The maximum VSWR of the circuit was 1.65:1.

C. STABILITY

The dc band edge oscillations are instabilities which occur either because of regenerative gain effects at or near the upper band edge (BL 2) of the circuit as a result of large, backward wave generated power on the circuit, or because of resonant trapped energy on the circuit caused by poor circuit matches in the region of circuit cutoff frequency. In broadband tubes, there is little margin between velocities associated with synchronous interaction at the band edge frequencies and those required for interaction over the operating band.

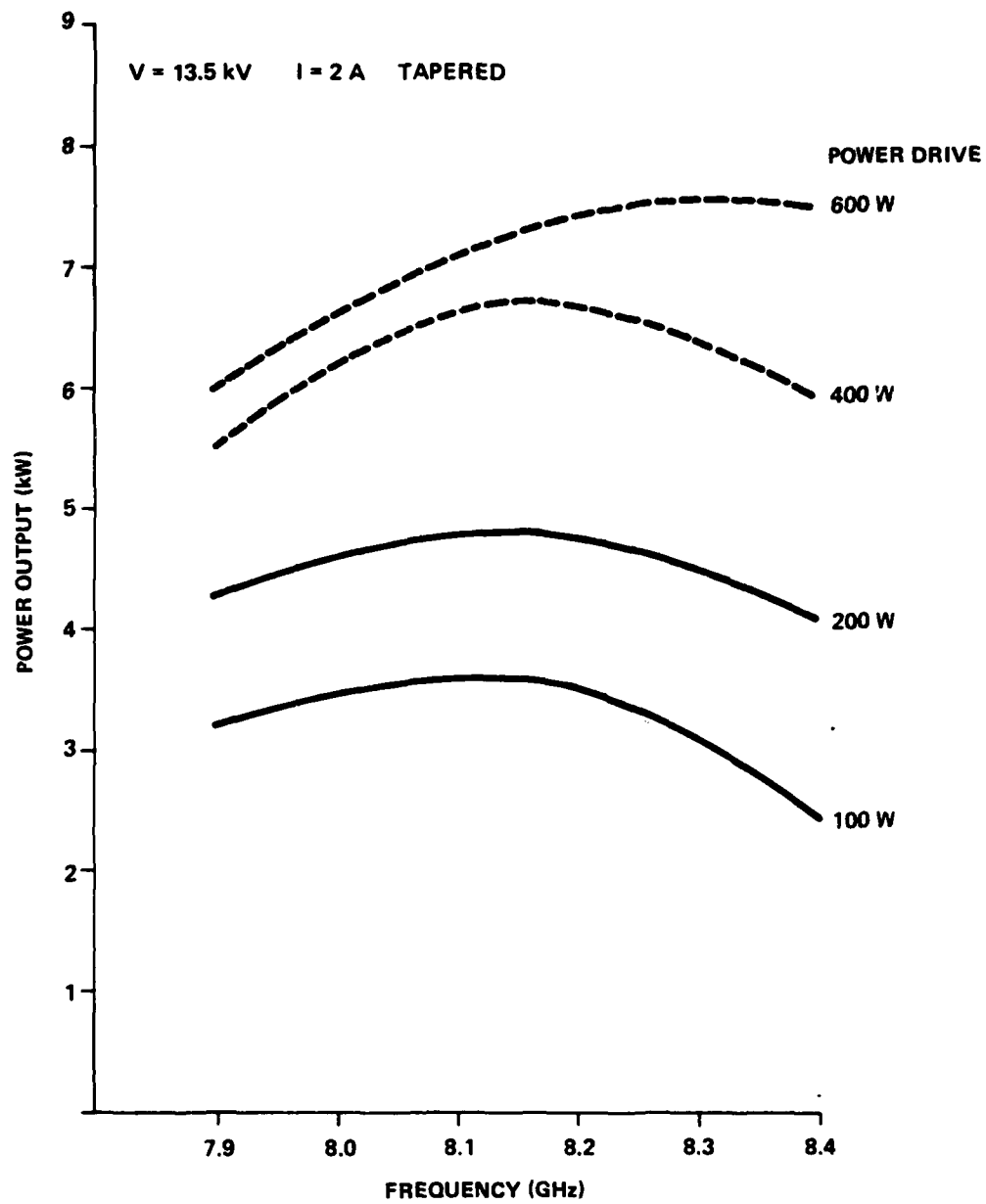


Figure 3. Twelve-Cavity Design – Power vs Frequency

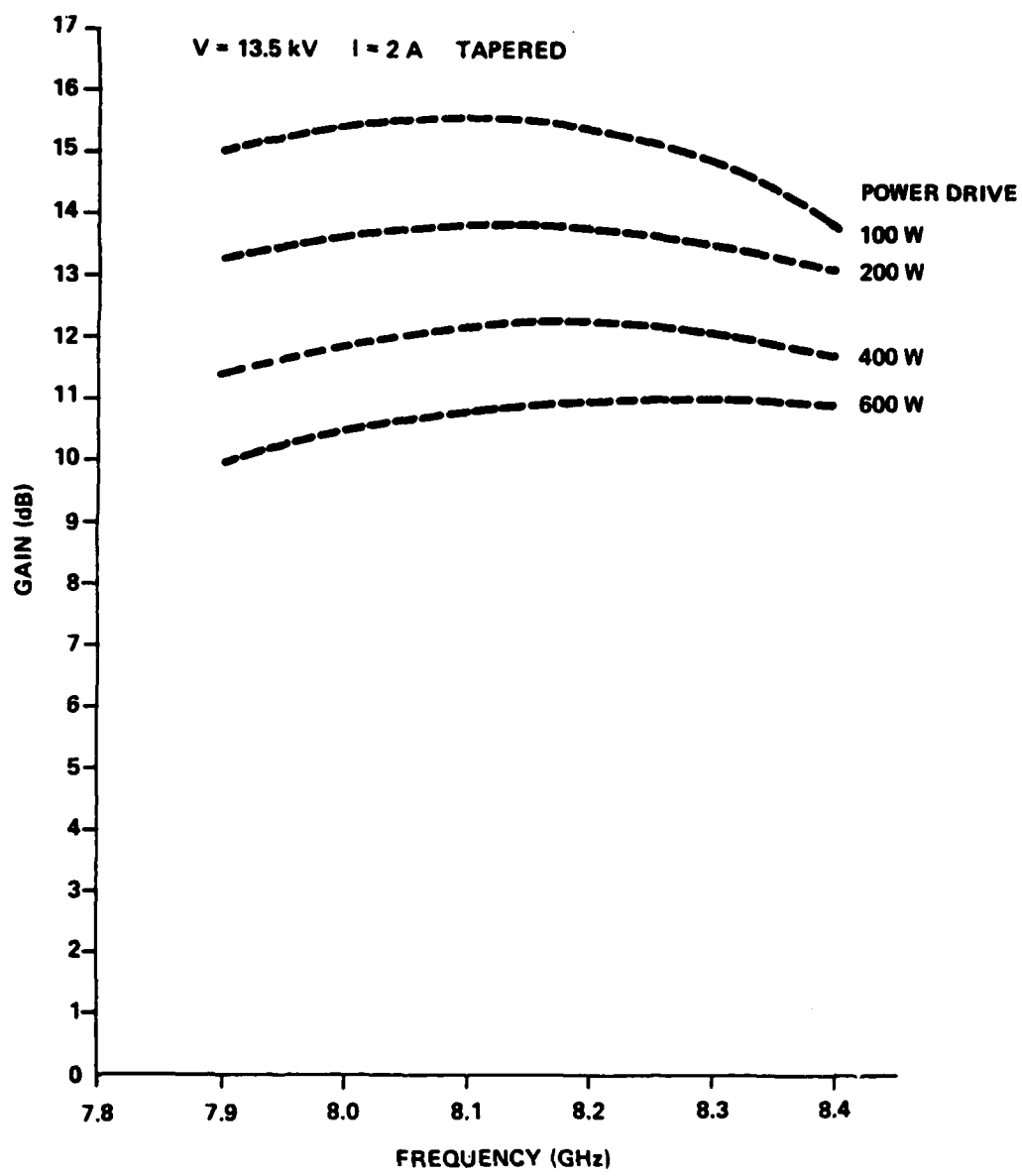


Figure 4. Twelve-Cavity Design – Gain vs Frequency

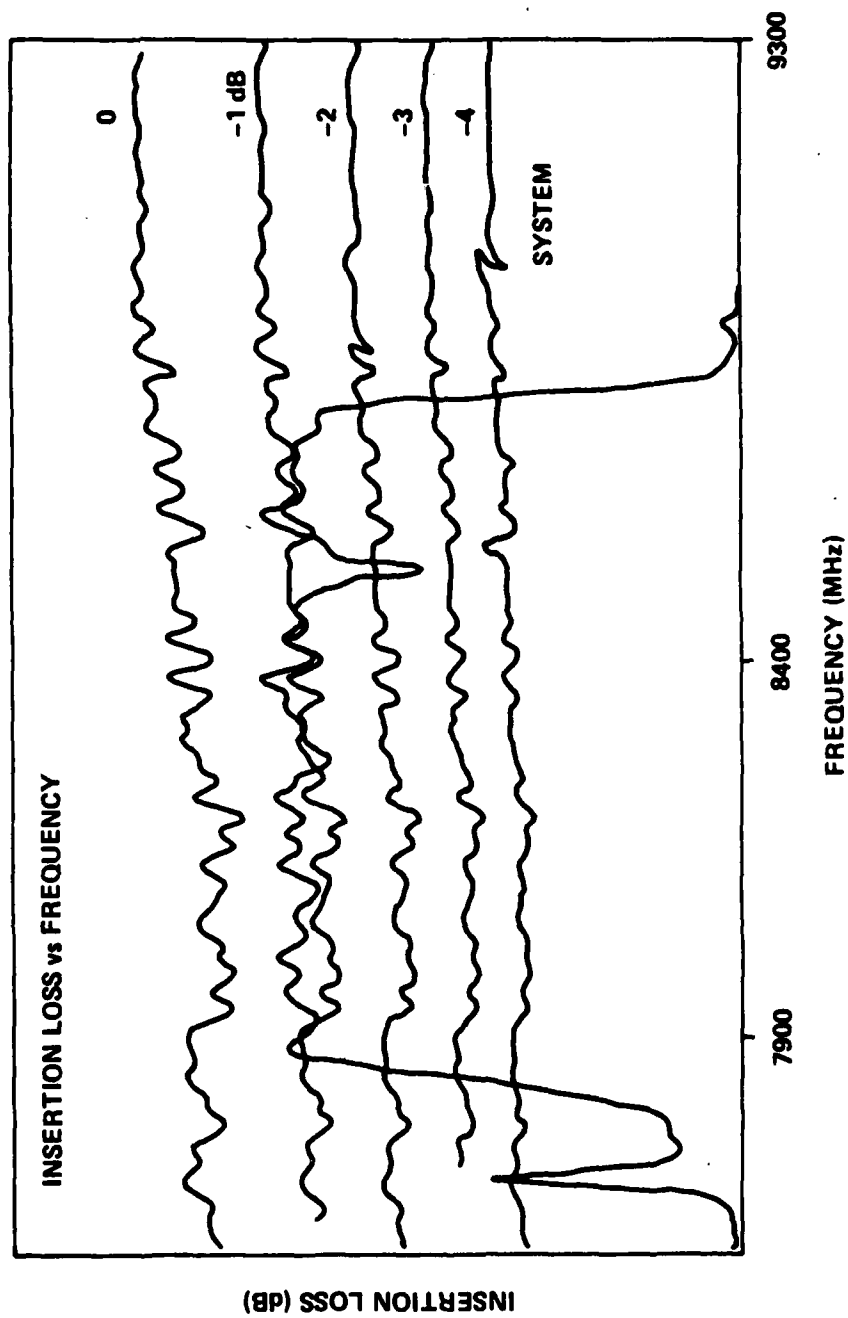


Figure 5. *Transmission Insertion Loss*

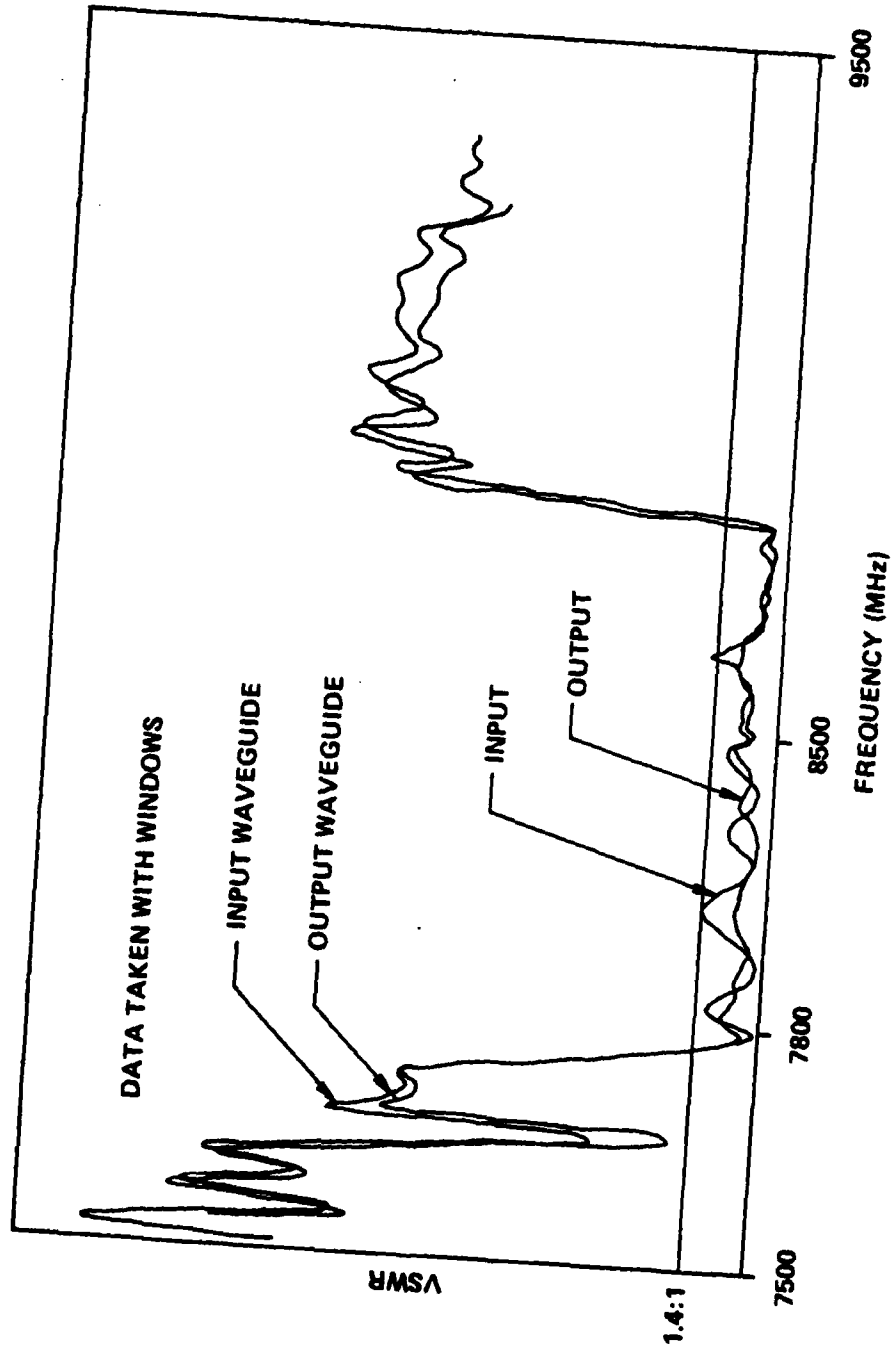


Figure 6. Match Data

The band edge oscillation usually manifests itself as a monotron-type oscillation which requires the total loop gain of a uniform circuit at the band edge frequencies. At these frequencies, which are the upper cutoff of the operating mode, the group velocity of the circuit is approaching zero, and the impedance of the circuit is going to infinity. Usually, these oscillations are suppressed at the operating voltage and current by use of distributed loss within the circuit, limiting the gain of the circuit and judiciously choosing the number of lossless cavities in the output section without too severely compromising the efficiency.

Another type of oscillation problem which tends to plague high efficiency, coupled cavity TWTs is an oscillation which is associated with high levels of rf drive. This oscillation is commonly referred to as a drive-induced oscillation. This instability occurs at or near saturated output power conditions, and the oscillation frequency is, again, at the band edge frequency. Because these instabilities only seem to occur at or near saturation, it was deduced that these oscillations must be associated with large-signal effects within the tube. This means that the oscillation must originate at the output end of the output circuit. Experiments on different tube types have borne out this hypothesis.

The output circuits of coupled cavity TWTs are usually designed to have a lossy and a lossless cavity section within the same circuit for reasons previously stated. These cavity sections, by design, have the same upper cutoff frequency. The lossy section of the circuit results in an impedance mismatch to the lossless section of the circuit, thereby reflecting the band edge frequency. This reflection may be canceled in cold matching the circuit by introducing another mismatch in the output line. Although the sum of these reflections might show, on a cold test basis, that the circuit appears well terminated at the band edge frequency, a trapped mode exists within the circuit. At this high Q trapped mode frequency, the lossless section of the circuit now appears similar to an extended interaction klystron. When the TWT is operated at or near saturation, enough slow electrons are produced by large signal velocity spread in the beam to be synchronous with the trapped mode and cause the rf oscillations.

The booster tube was designed by specifically limiting the gain of the circuit at the upper band edge so that the tube would be dc stable at the operating voltage and current without the use of loss. Further, the design of the upper cutoff frequency characteristics of the circuit is such that the large signal cavities near the output of the tube would be well terminated in both directions of the circuit without trapping modes and lowering the Q_{ext} of the band edge frequency.

Stability calculations on the twelve- and fourteen-cavity design were carried out. Figure 7 shows the results of these calculations. The calculation is made by computing the minimum start oscillation current for a fixed voltage. Figure 7 shows that the tube design has adequate margin at the operating voltage of 13 kV at 2 A of beam current. The calculations further show that the tube should not oscillate above 9.5 kV.

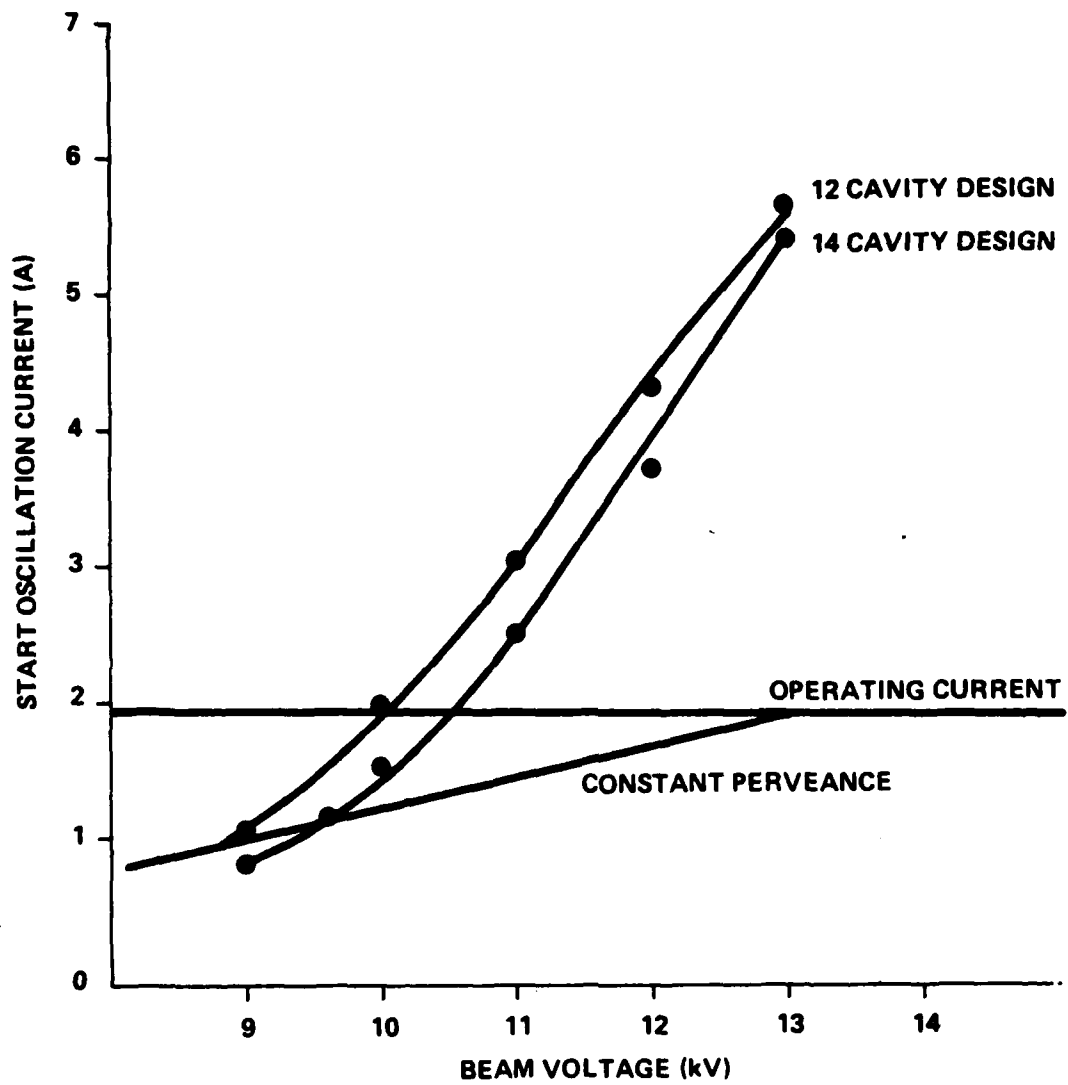


Figure 7. Stability Calculations, 12- and 14-Cavity Design

III. TEST DATA

Because of the unavailability of a broadband 500 W power source to test the tube, a klystron drive source which was tuned in 100 MHz steps over the band was used.

The power output over the band was measured and presented, showing the drive power measured through the tube when the beam was turned off (Figures 8 through 12).

Gain characteristics of the tube at various frequencies were also measured showing the power output as a function of drive power (Figures 13 through 17).

Amplitude data was also measured and plotted and the data is presented in steps of 100 MHz over the band (Figures 18 through 22). For the most part, it was found that the booster amplitude tracked with the amplitude of the driver.

An attempt was made to measure the phase characteristics of the booster. The measurements clearly showed that the booster introduced very little phase variation. The measurements indicated that the narrow band phase of the klystron was measured in all cases (see Figures 23 through 27). Finally, the stability of the booster was measured against the calculation.

Figure 28 shows the results of the measured stability data. The measurements showed that the start oscillation current for the tube was slightly lower than calculated for the various voltages, and the minimum operating oscillation has moved up from 9.5 kV to 10.5 kV. However, this left plenty of margin in the tube design, which operated at a minimum of 13 kV.

TABLE OF OPERATING PARAMETERS

Beam Voltage	13.2	kV
Beam Current	2.0	A
Ibody	10	mA
Heater Voltage	13.5	V
Heater Current	3.0	A
Solenoid Current	10	A
Solenoid Voltage	134	V
Body Flow	1.0	gpm
Solenoid Flow	2.0	gpm

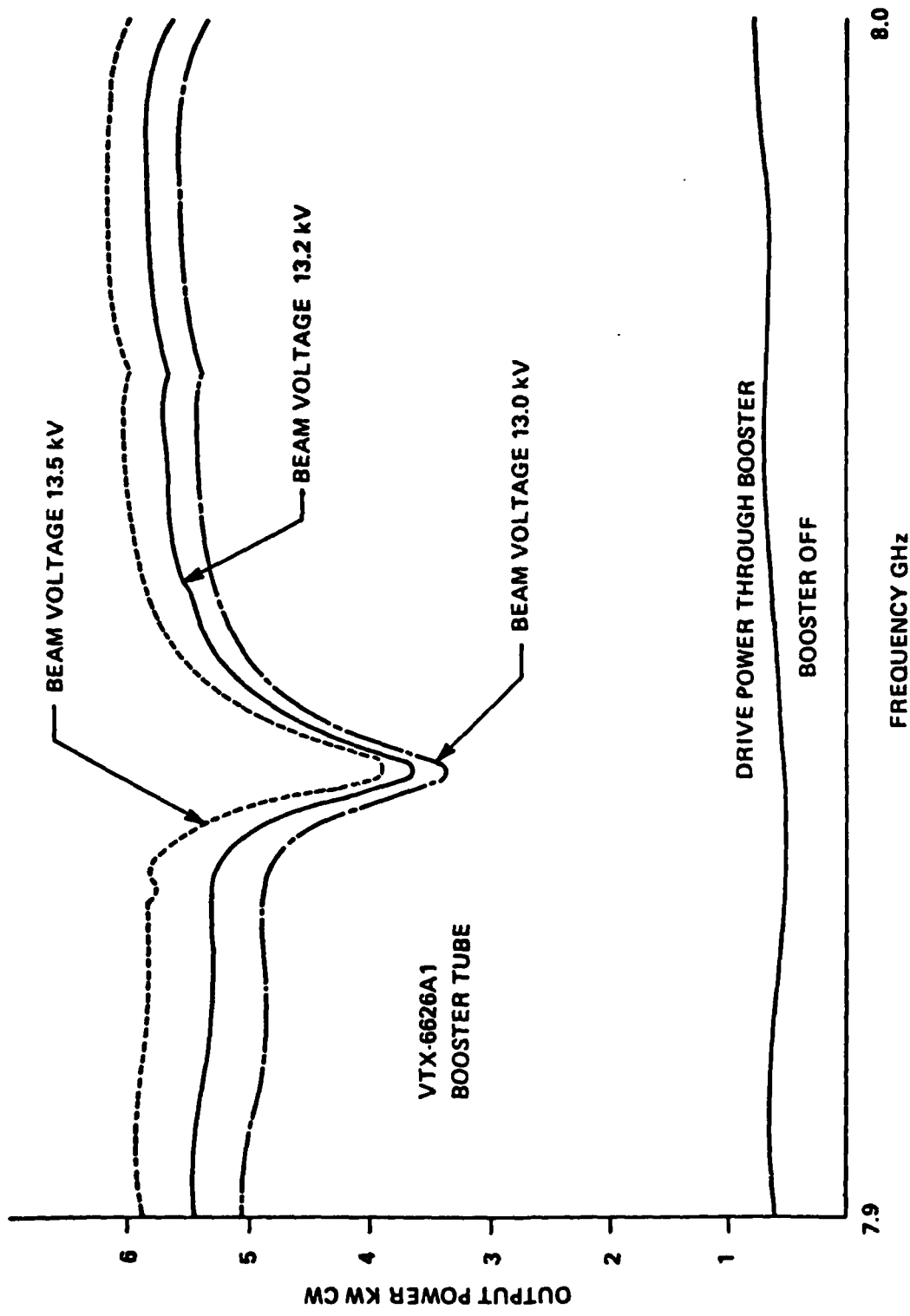


Figure 8. Output Power vs 7.9-8.0 Frequency

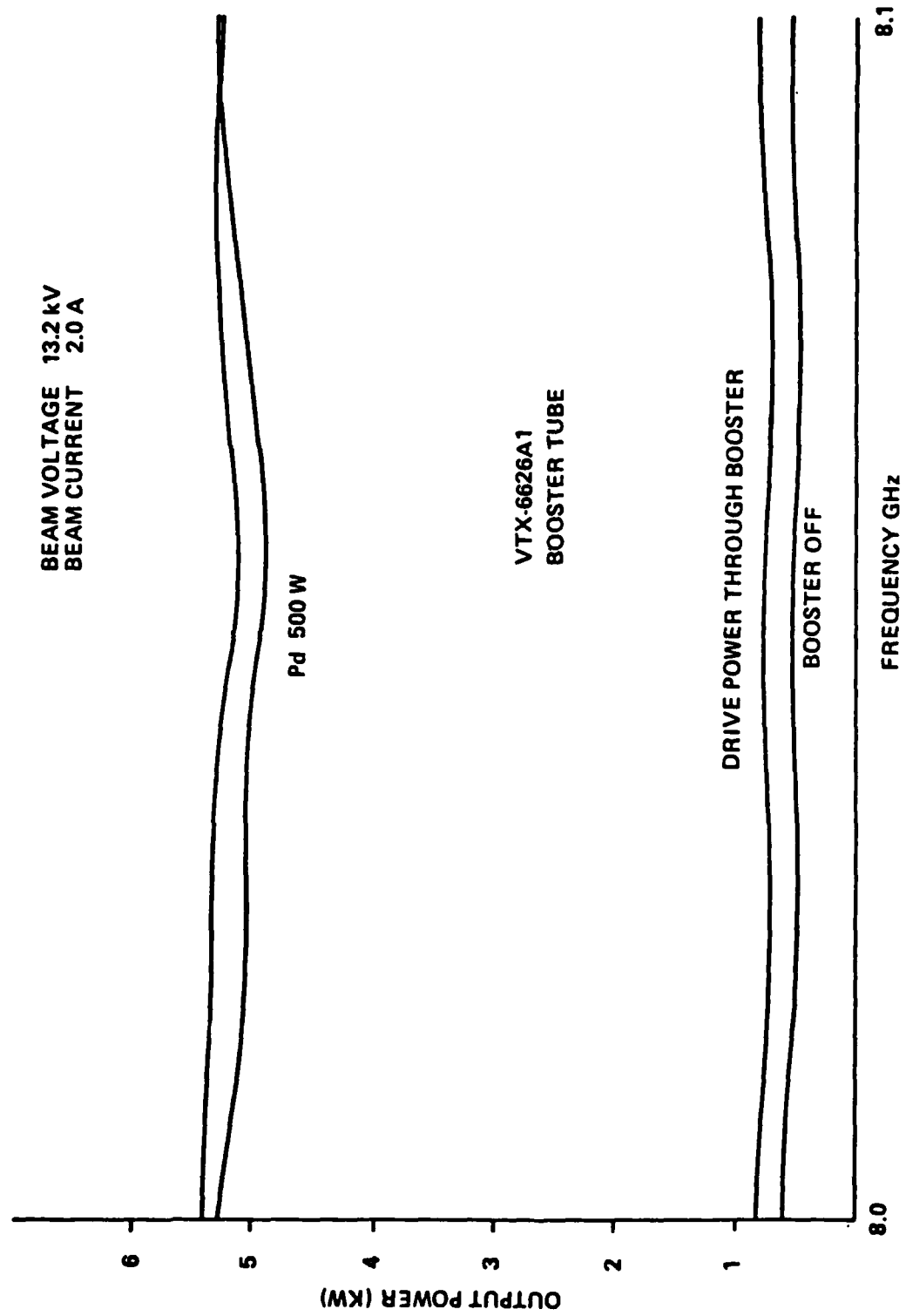


Figure 9. Output Power vs 8.0-8.1 Frequency

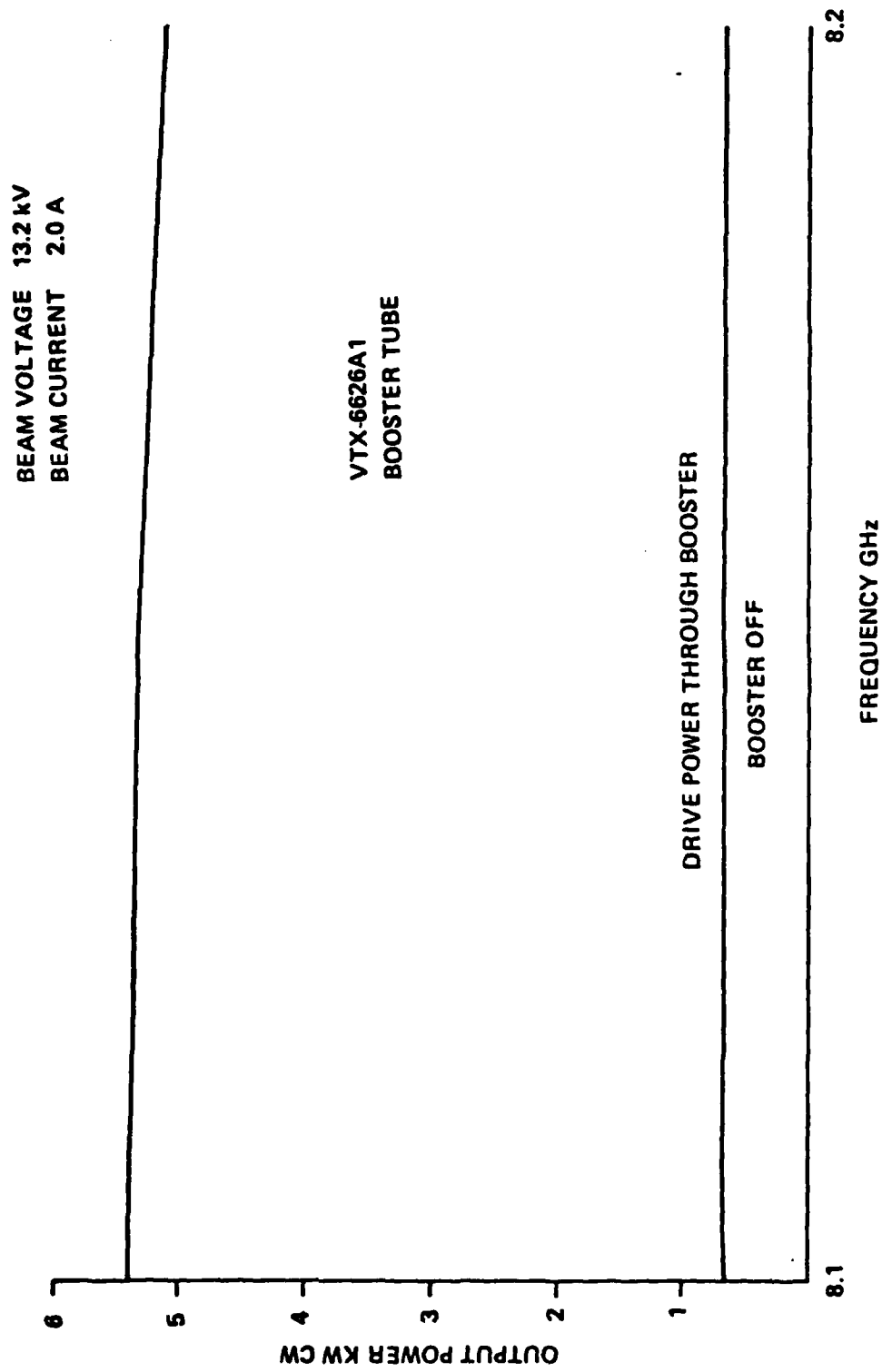


Figure 10. Output Power vs 8.1-8.2 Frequency

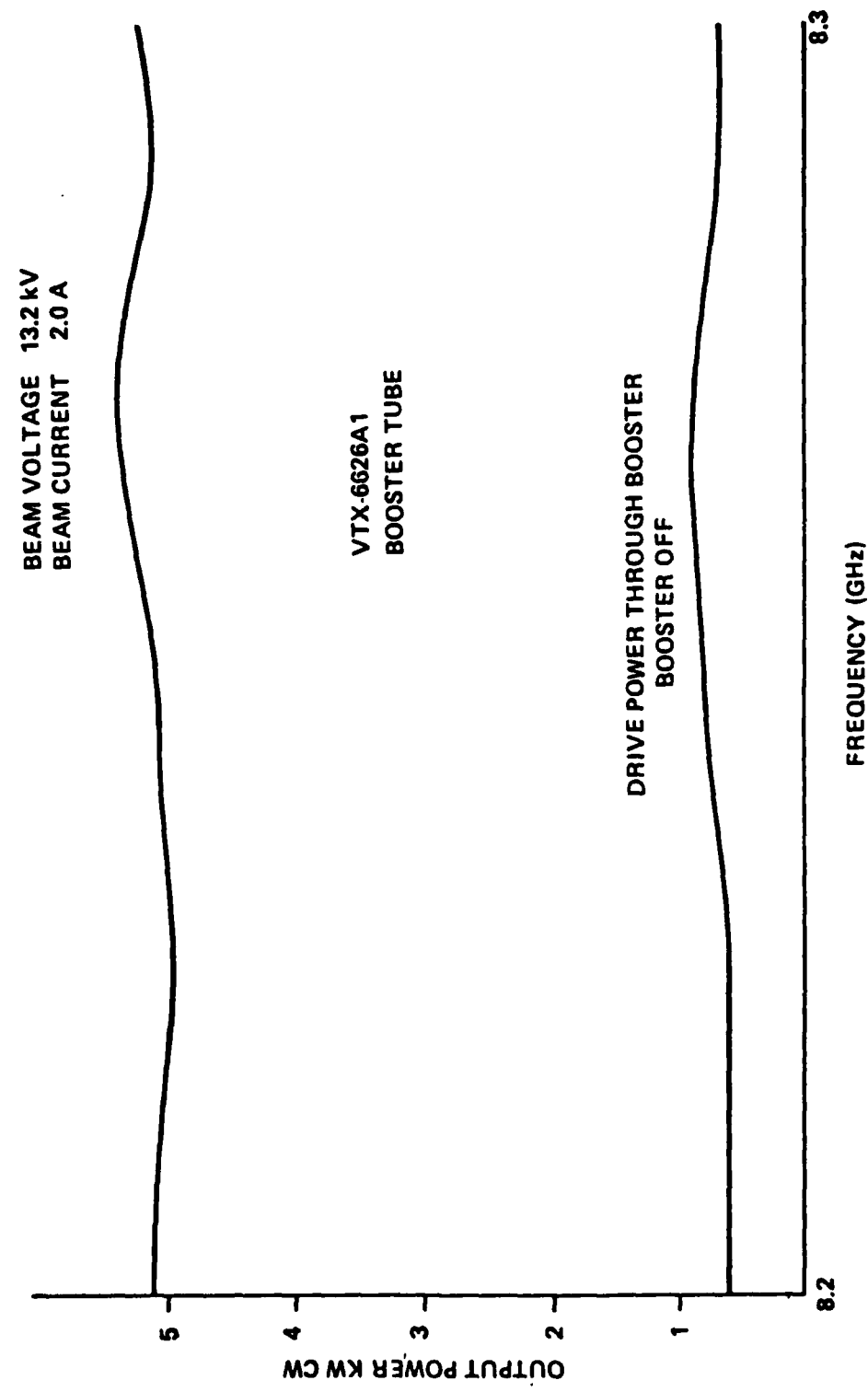


Figure 11. Output Power vs 8.2-8.3 Frequency

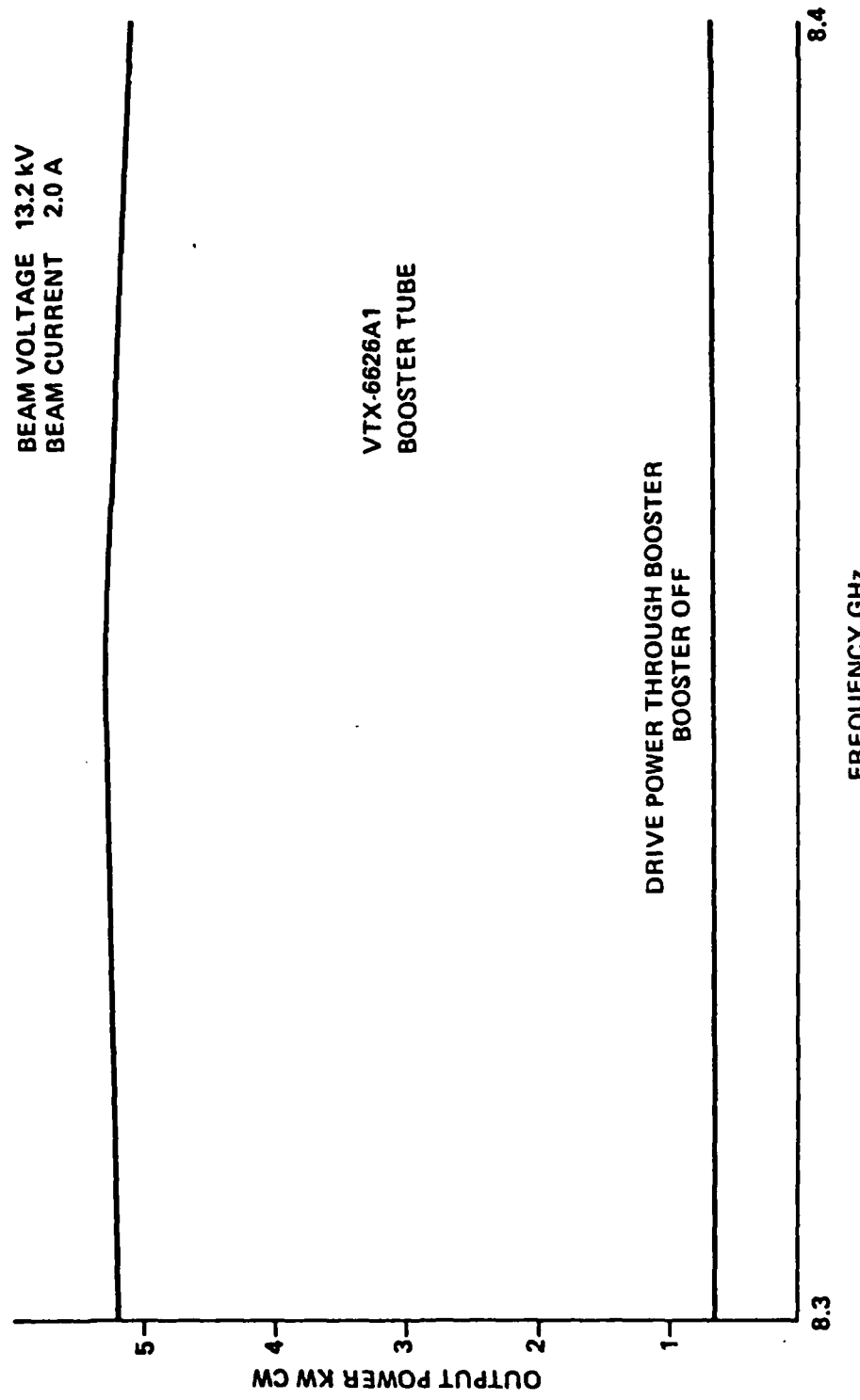


Figure 12. Output Power vs 8.3-8.4 Frequency

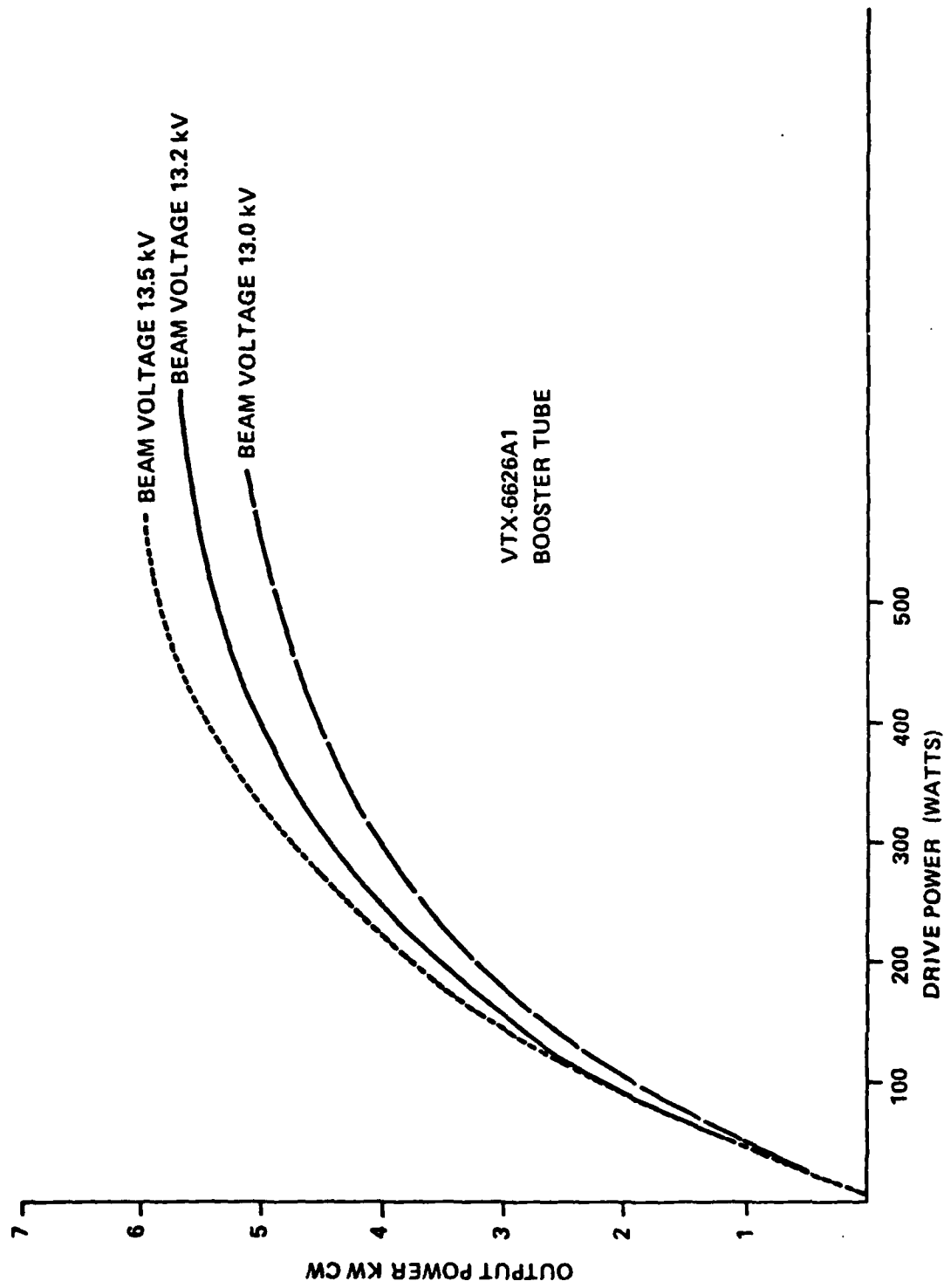


Figure 13. Power Output vs Power Drive - 7.9 GHz

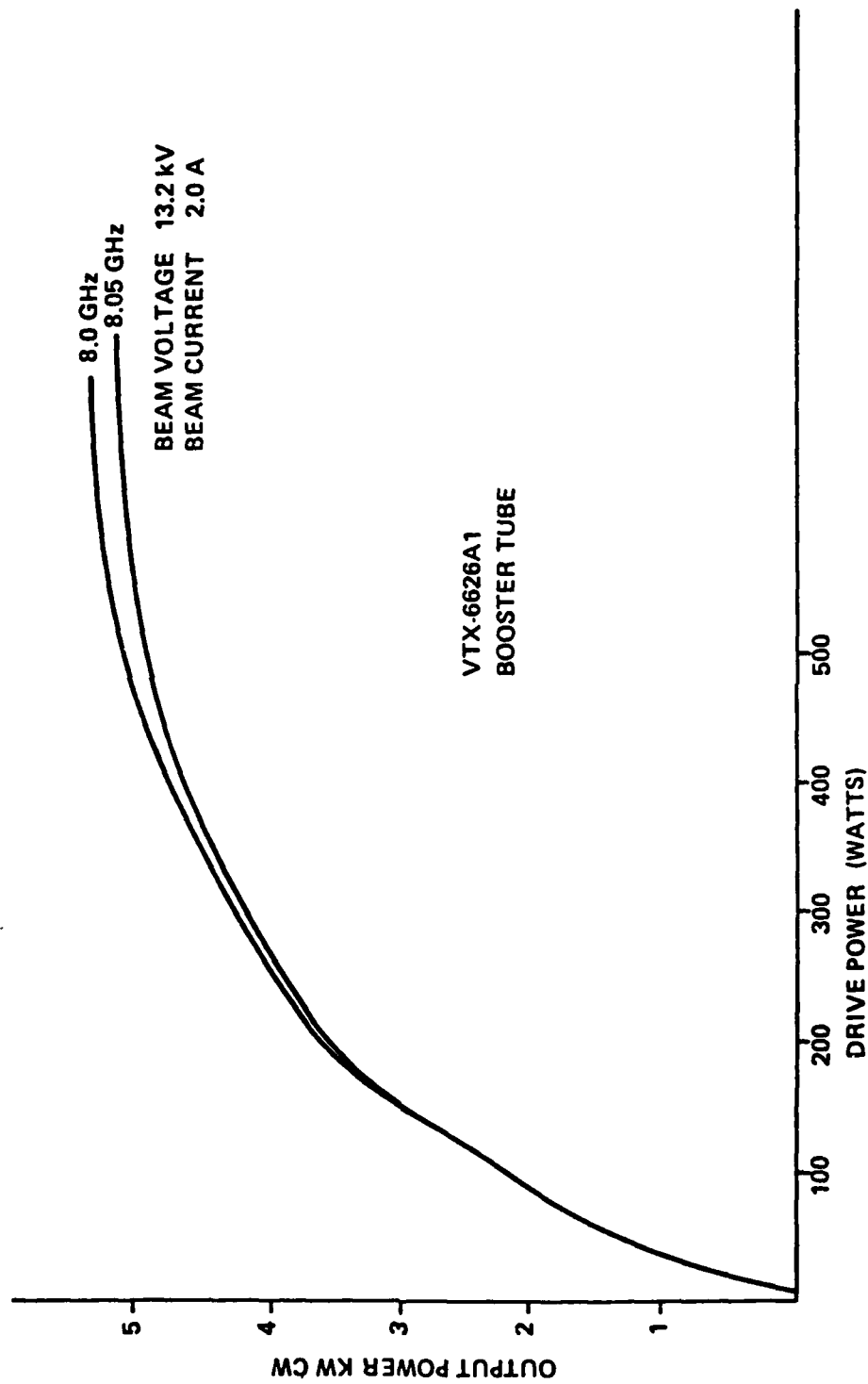


Figure 14. Power Output vs Power Drive - 8.0 - 8.05 GHz

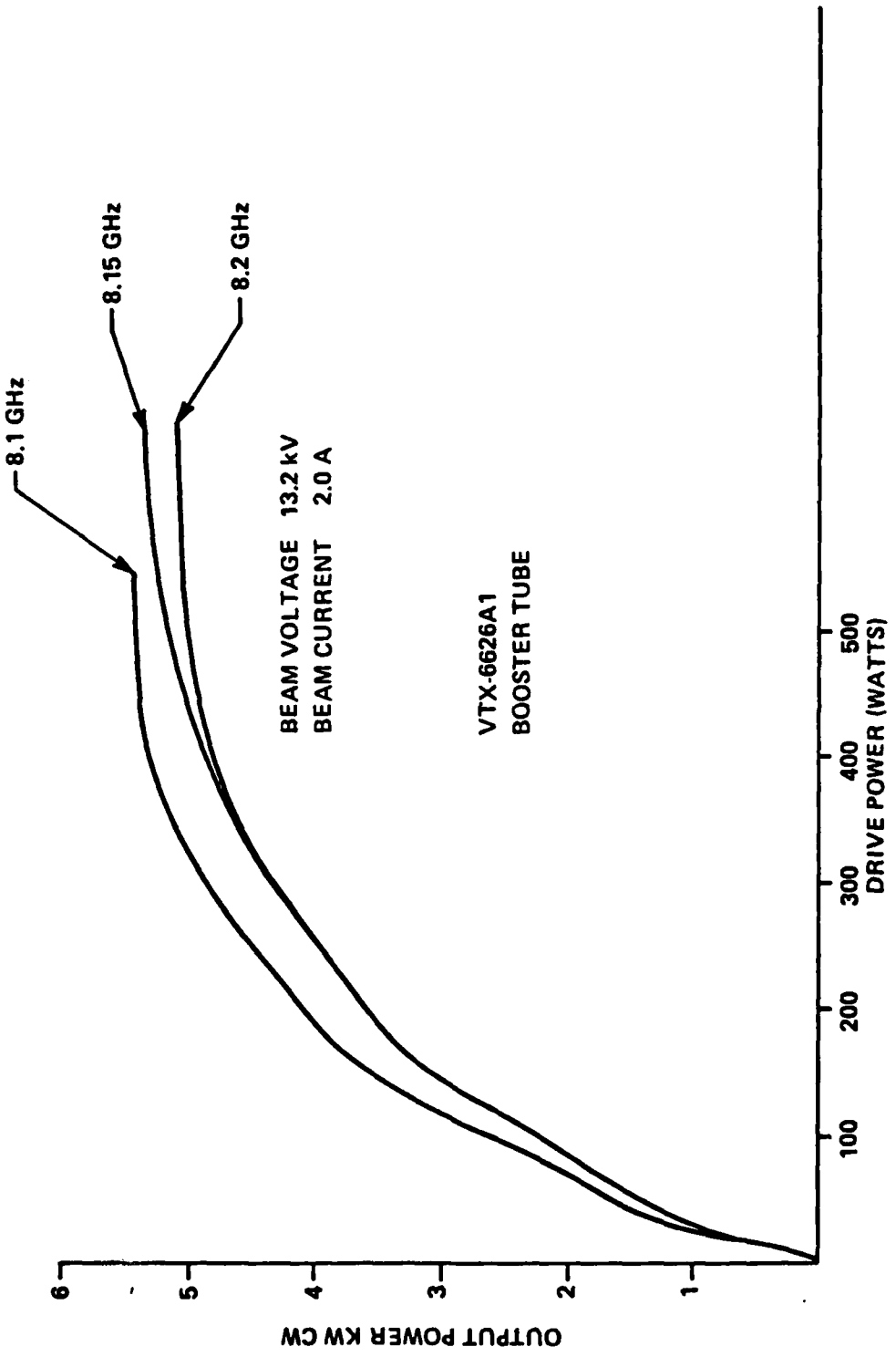


Figure 15. Power Output vs Power Drive – 8.1, 8.15, 8.2 GHz

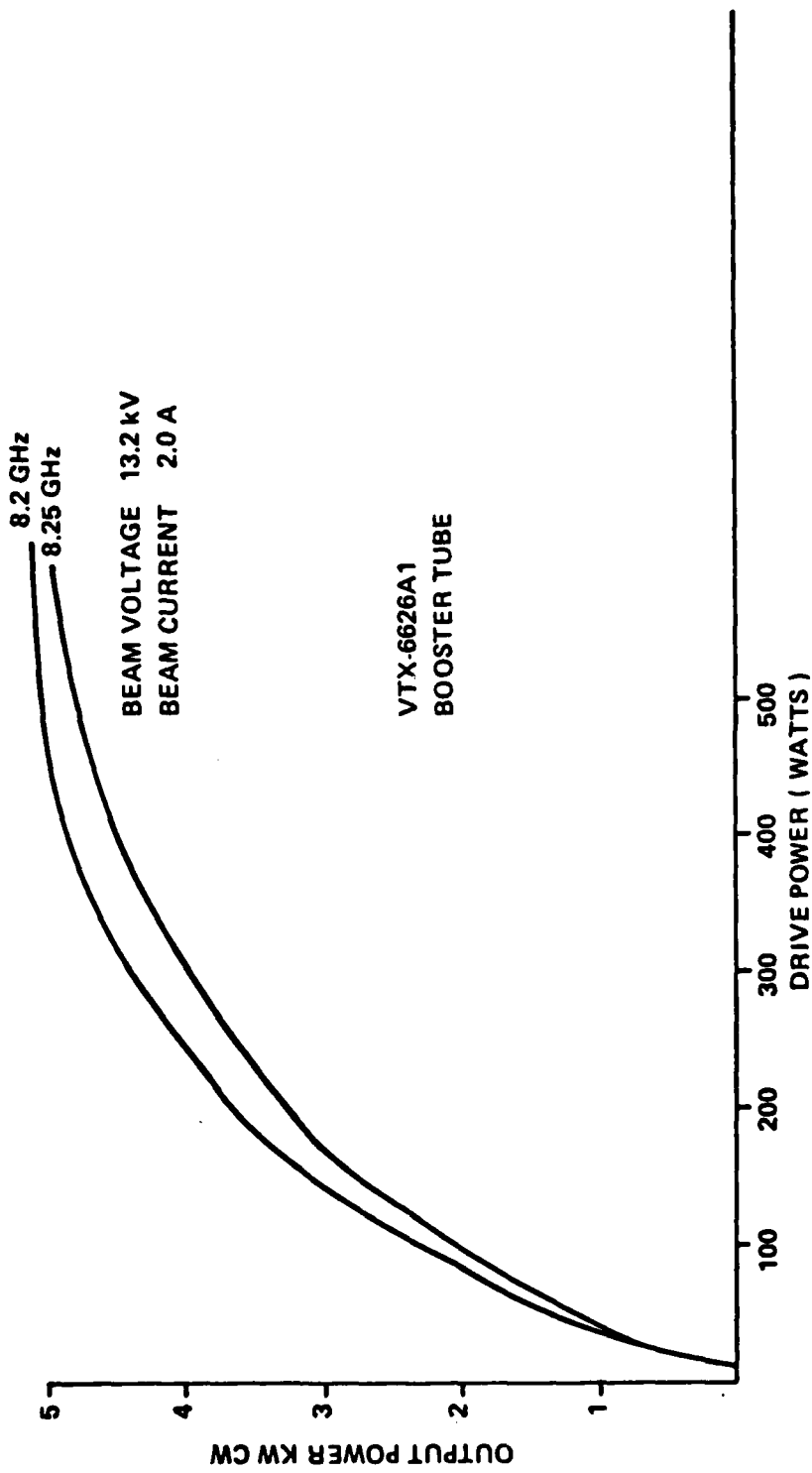


Figure 16. Power Output vs Power Drive – 8.2, 8.25 GHz

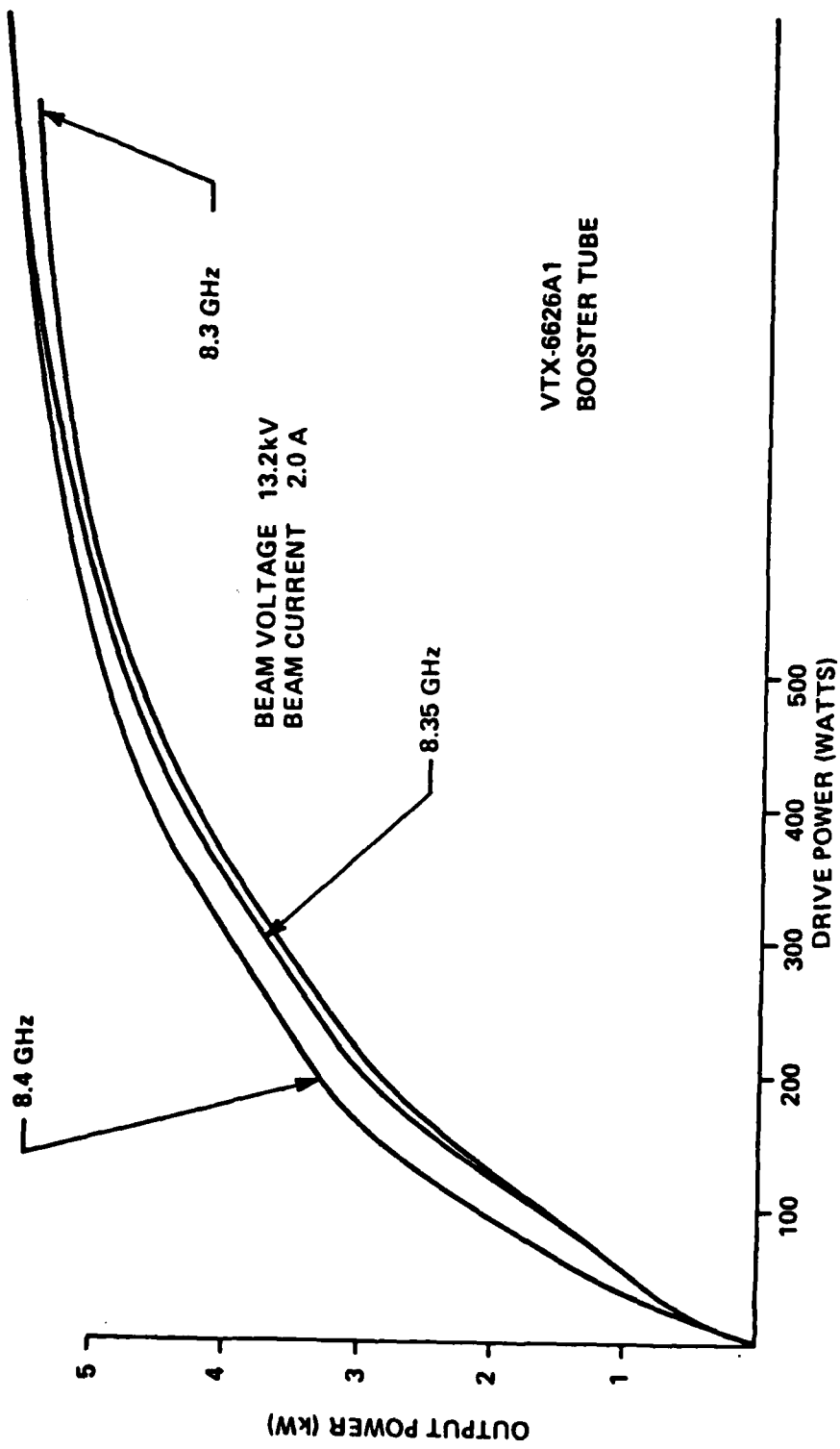


Figure 17. Power Output vs Power Drive – 8.3, 8.35, 8.4 GHz

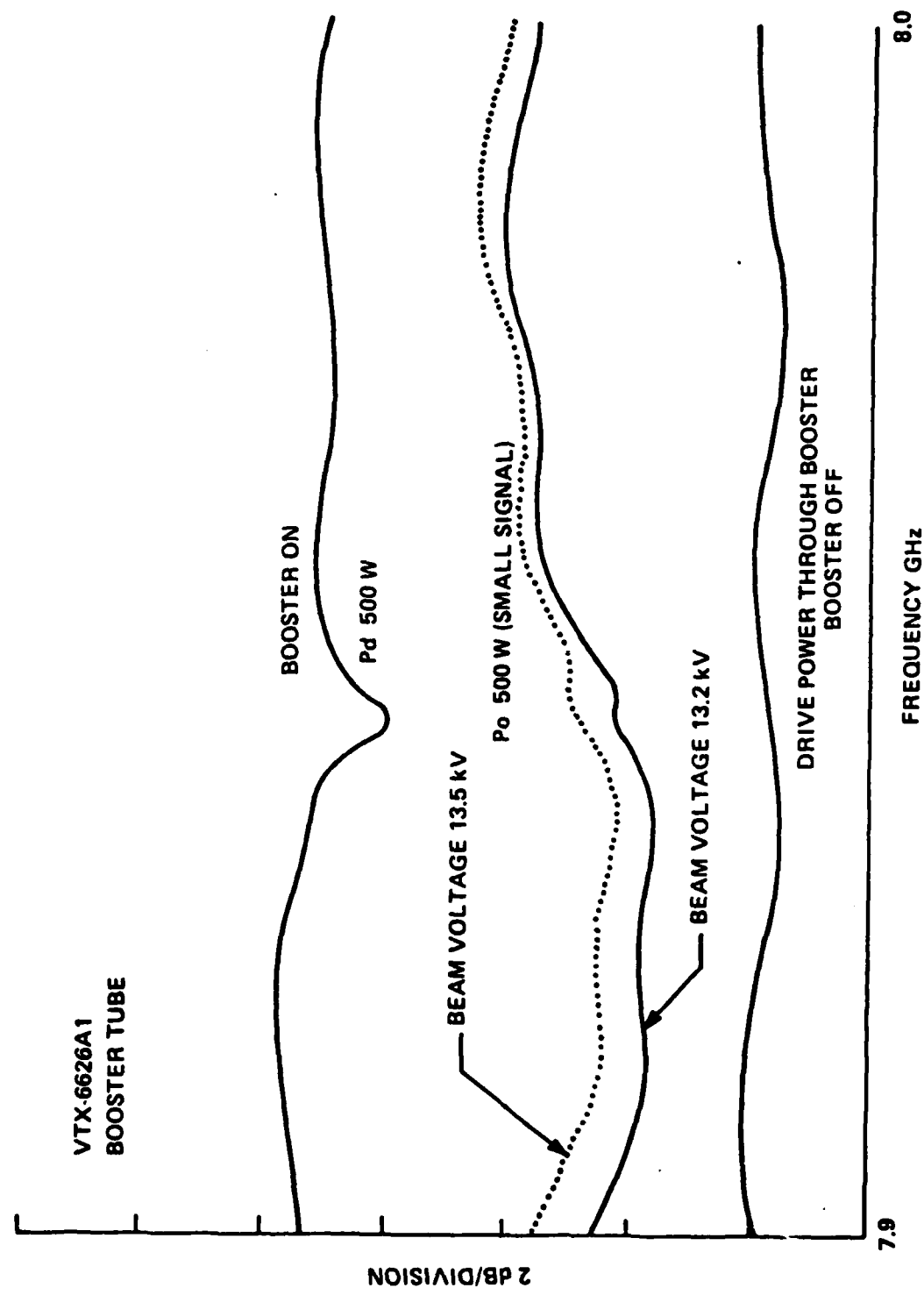


Figure 18. Booster Amplitude Measured with Klystron Driver 7.9 - 8.0 Frequency

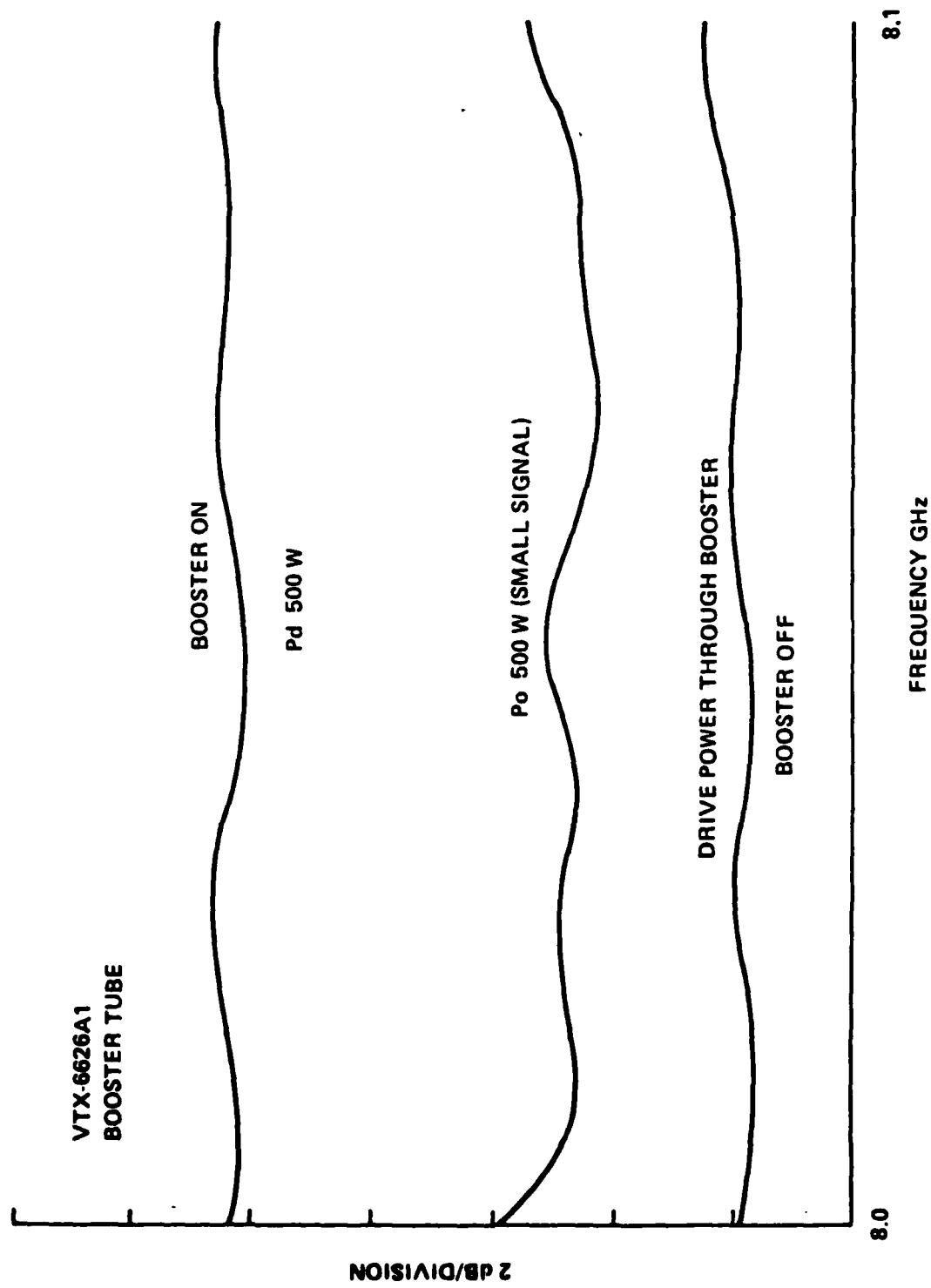


Figure 19. Booster Amplitude Measured with Klystron Driver 8.0 – 8.1 Frequency

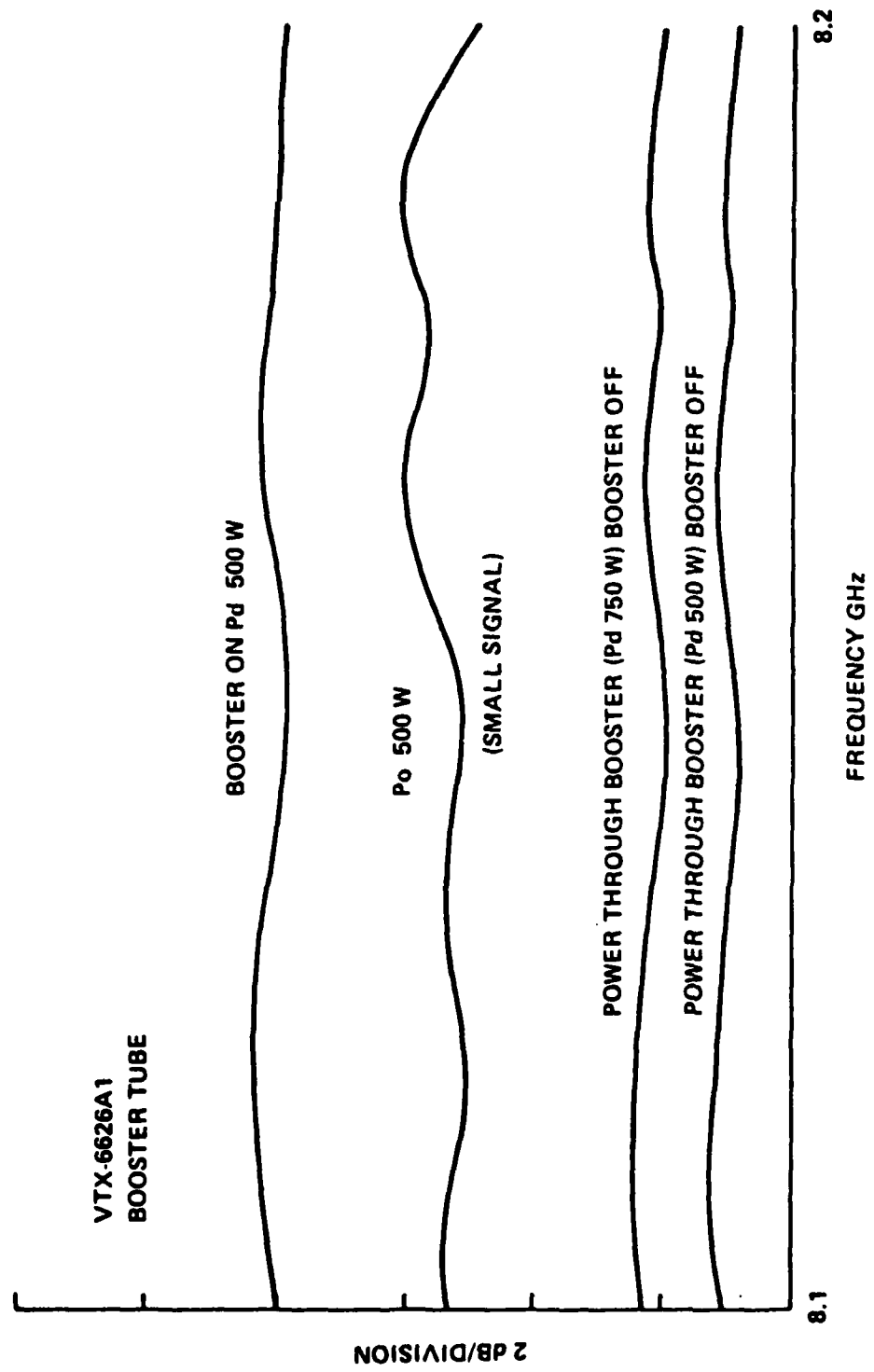


Figure 20. Booster Amplitude Measured with Klystron Driver 8.1 – 8.2 Frequency

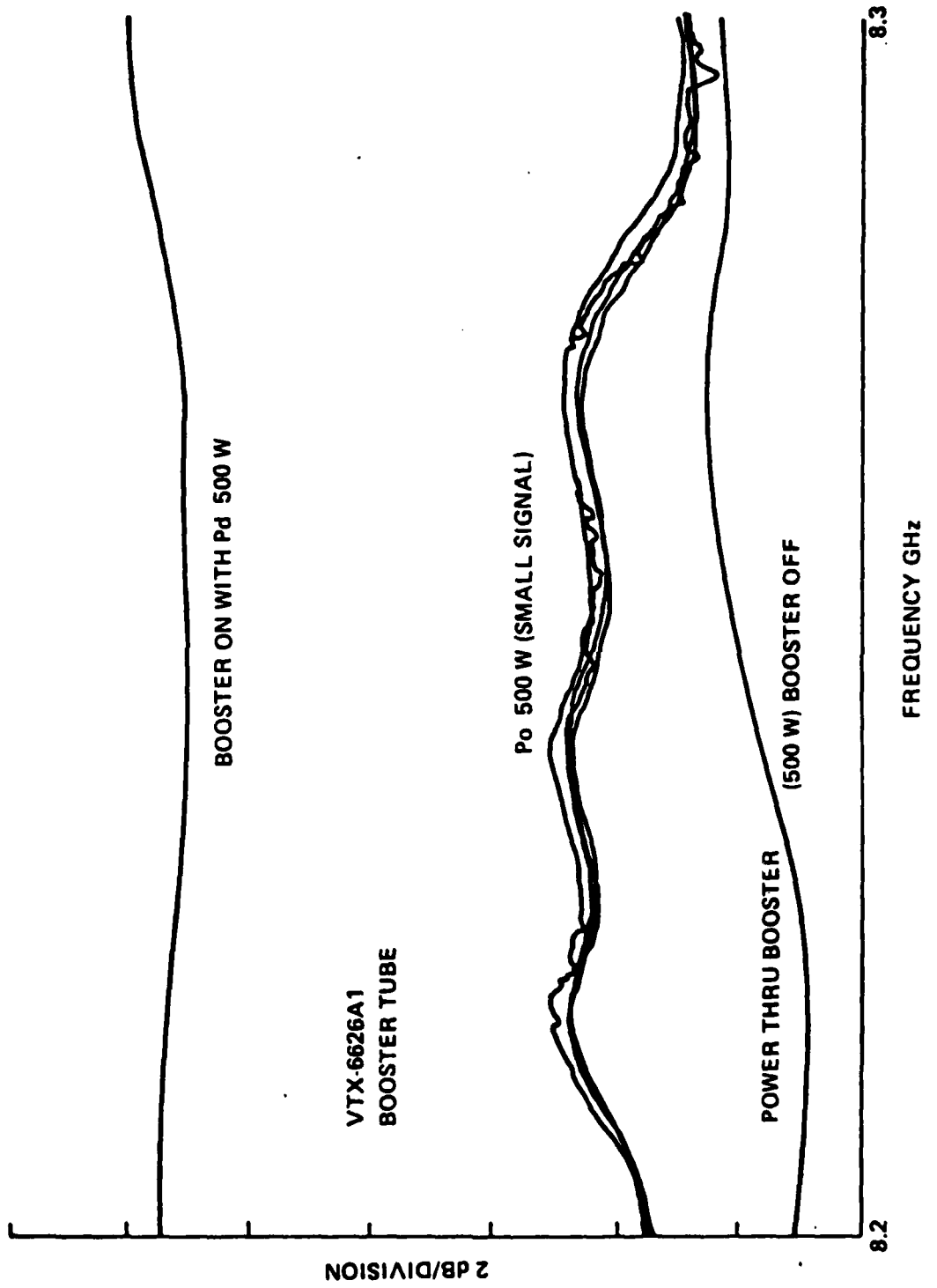


Figure 21. Booster Amplitude Measured with Klystron Driver 8.2 – 8.3 Frequency

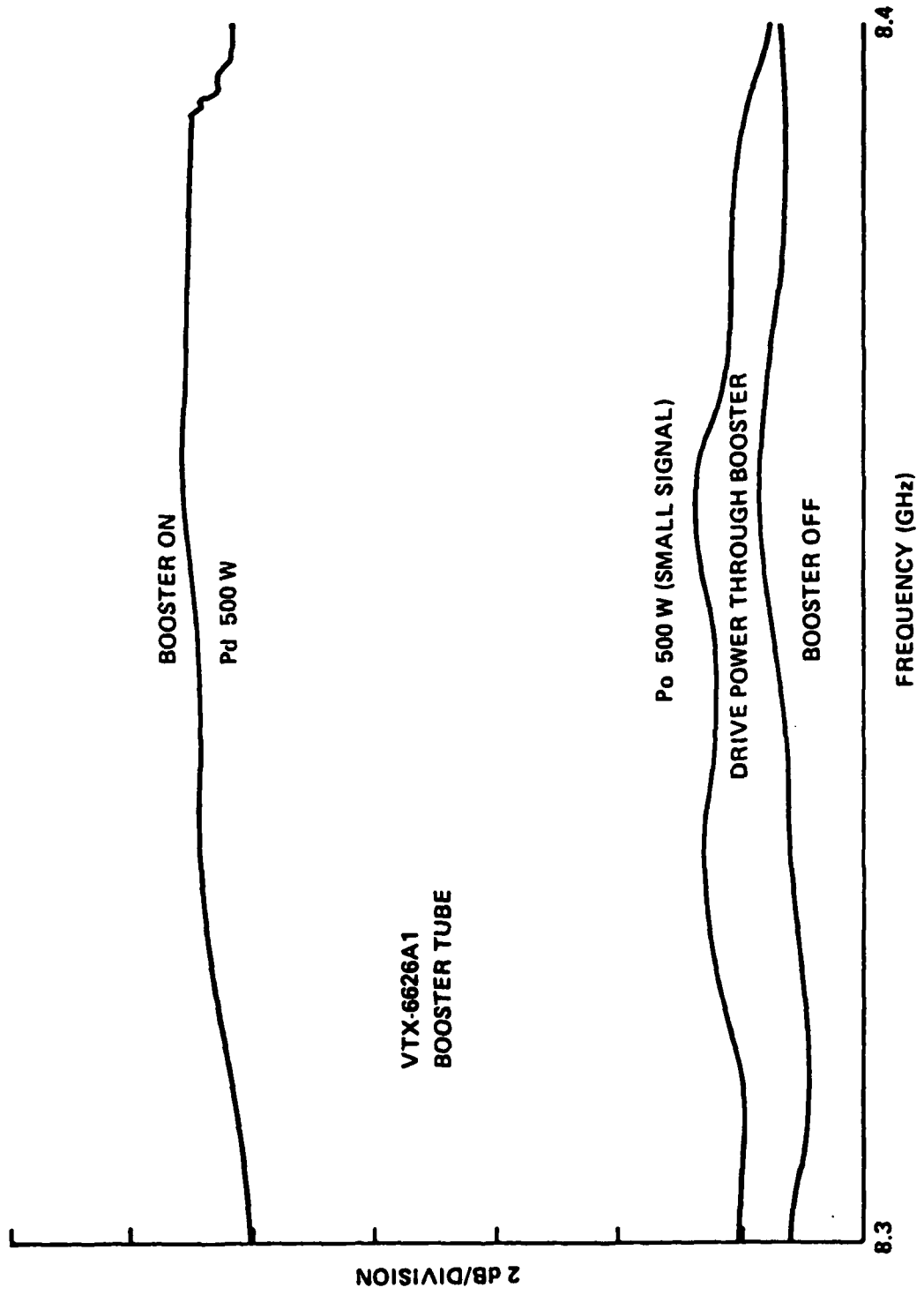


Figure 22. Booster Amplitude Measured with Klystron Driver 8.3 – 8.4 Frequency

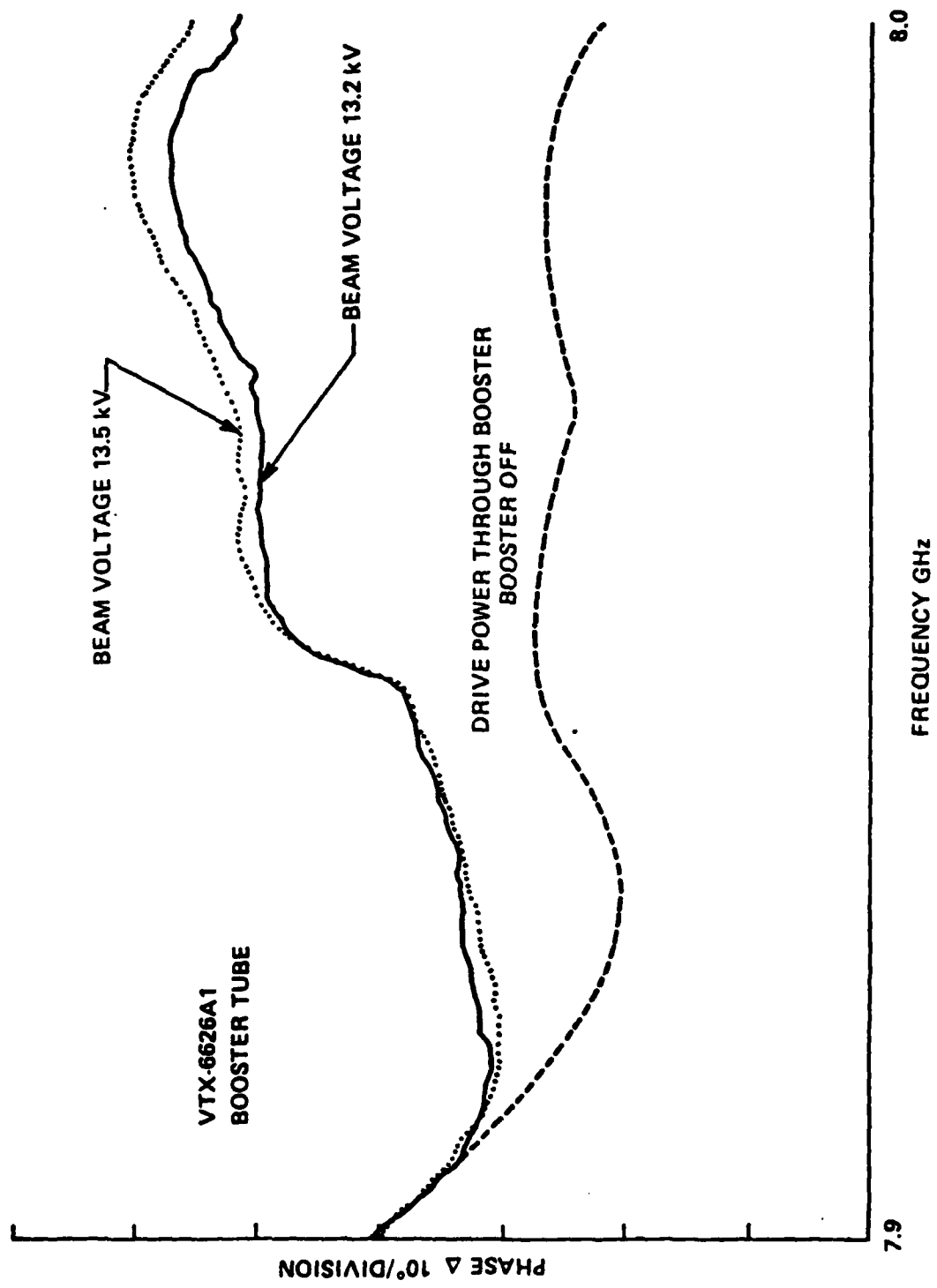


Figure 23. Booster Phase Deviation from Linearity Measured with Klystron Driver 7.9 – 8.0 Frequency

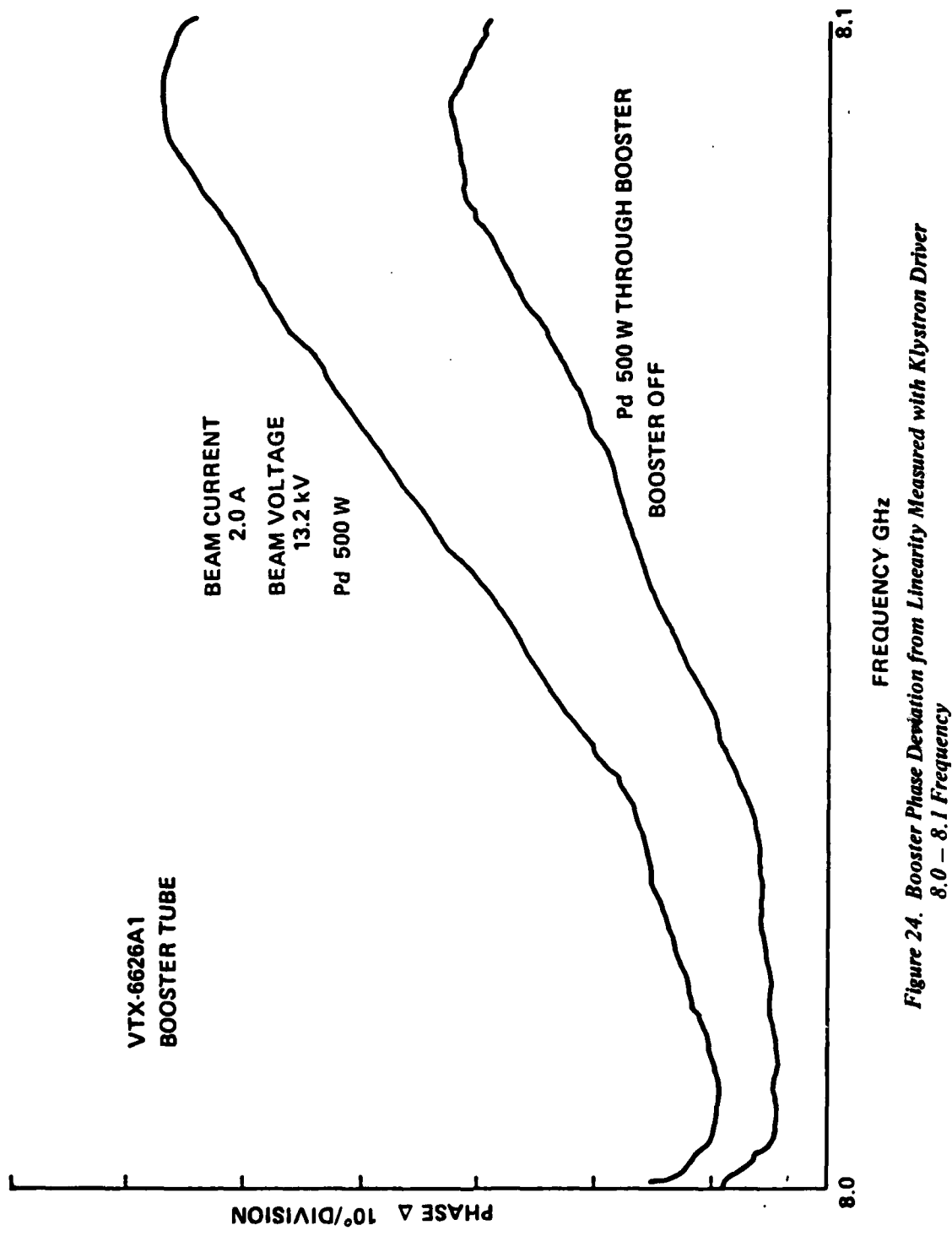


Figure 24. Booster Phase Deviation from Linearity Measured with Klystron Driver
8.0 – 8.1 Frequency

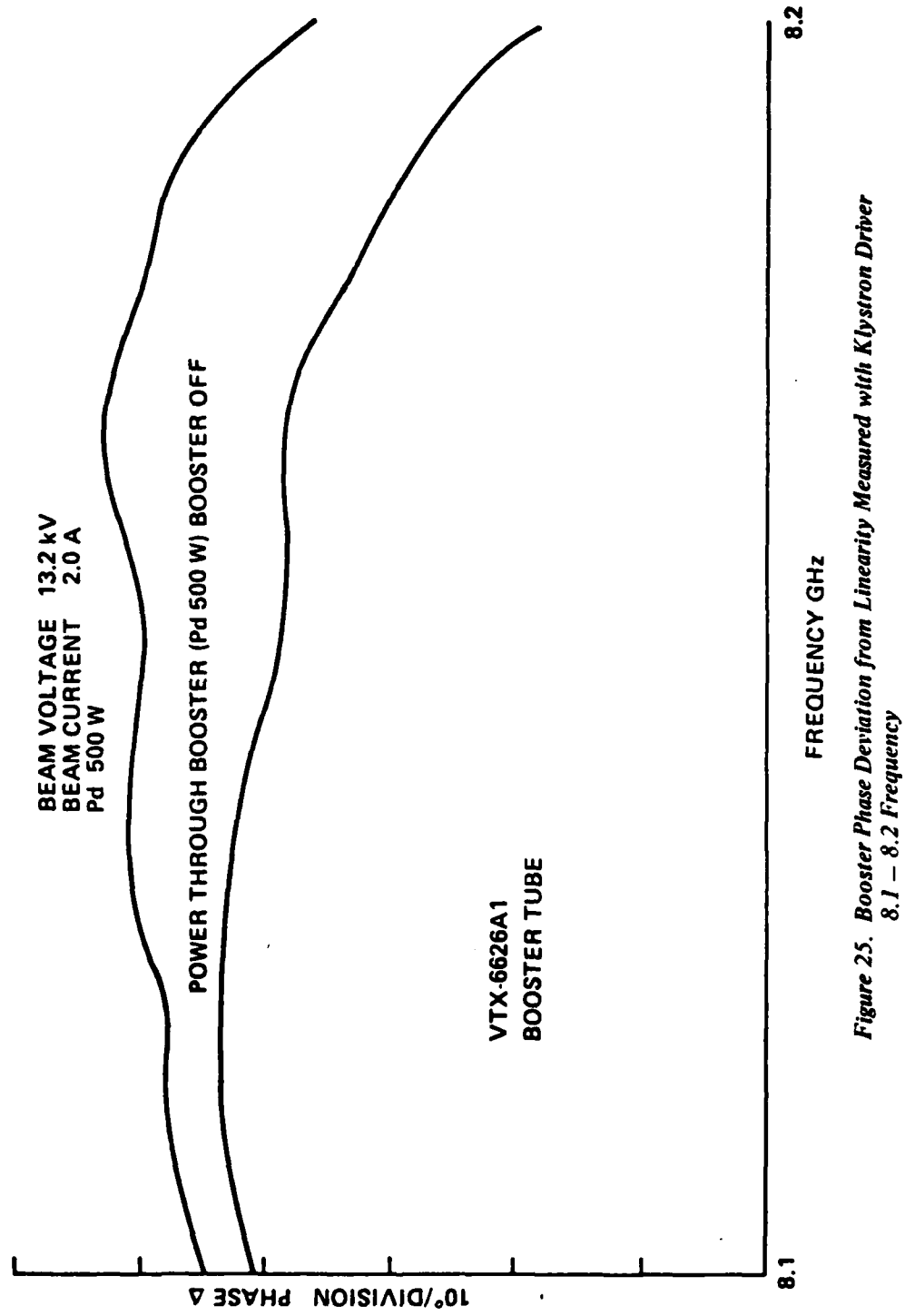


Figure 25. Booster Phase Deviation from Linearity Measured with Klystron Driver
8.1 – 8.2 Frequency

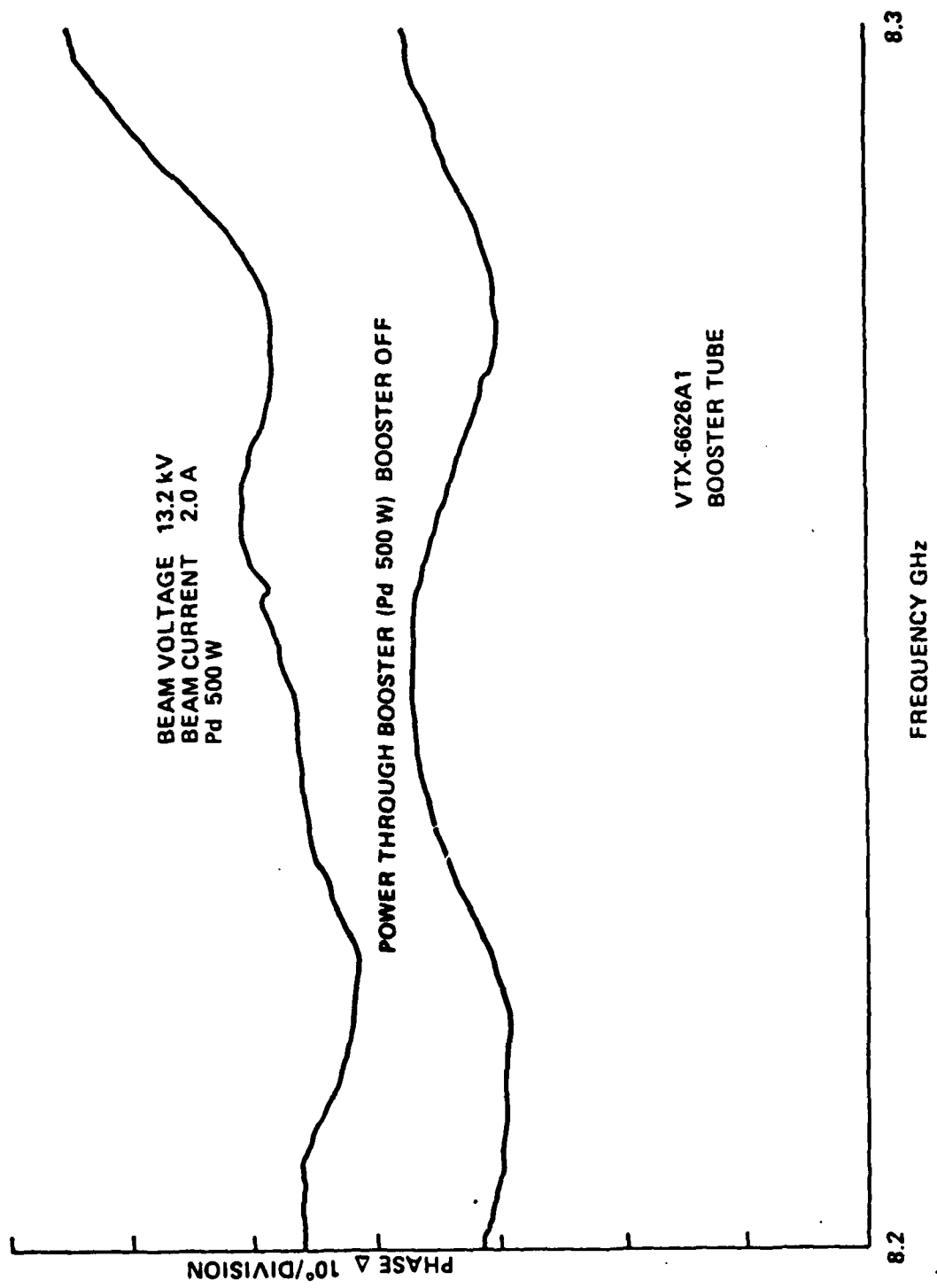


Figure 26. Booster Phase Deviation from Linearity Measured with Klystron Driver
8.2 – 8.3 Frequency

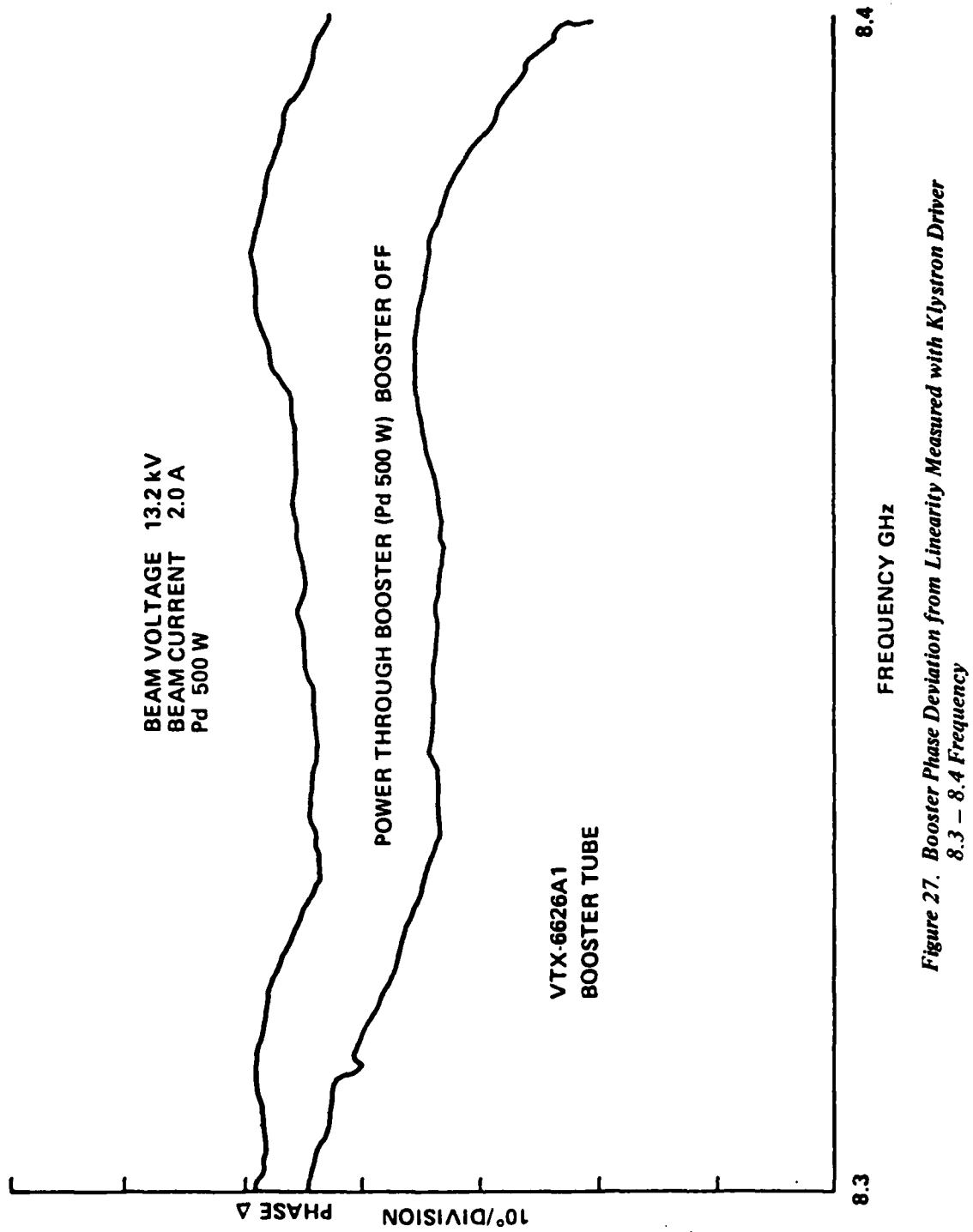


Figure 27. Booster Phase Deviation from Linearity Measured with Klystron Driver
8.3 – 8.4 Frequency

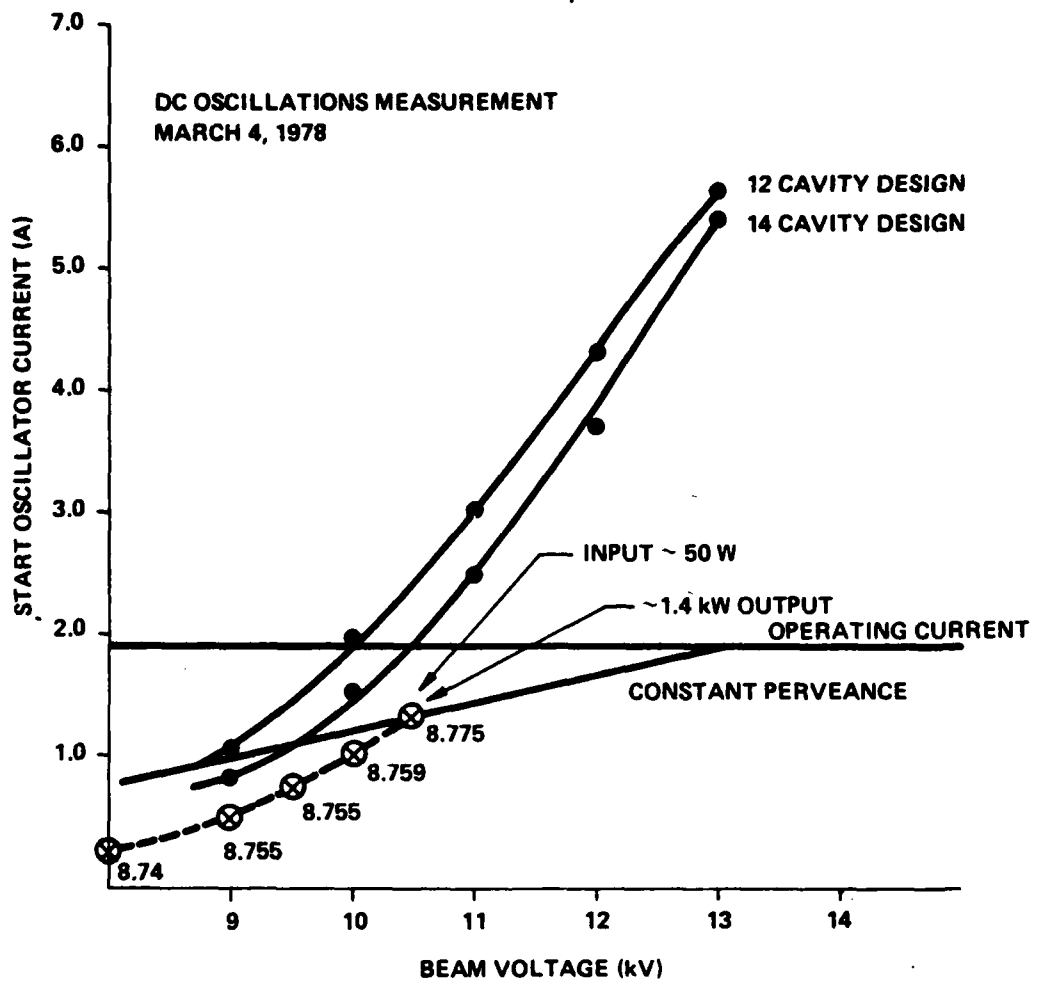


Figure 28. Stability Calculations